

NASA CR 54961
AGC 8800-64

SUMMARY OF MATERIALS
TECHNOLOGY OF M-1 ENGINE

By

G. R. Janser

Prepared for

National Aeronautics and Space Administration

GPO PRICE \$ _____

Contract NAS 3-2555

(STI PRICE(S) \$ _____

Hard copy (HC) # 2.50

Microfiche (MF) .75



AEROJET-GENERAL CORPORATION

SACRAMENTO, CALIFORNIA

53 July 65

N66 33977

(THRU)	1	(CODE)	15
(CATEGORY)			
(ACCESSION NUMBER)	85	(PAGES)	CR-54961
(NASA CR OR TMX OR AD NUMBER)			

NOTICE

This report was prepared as an account of Government sponsored work. Neither the United States, nor the National Aeronautics and Space Administration (NASA), nor any person acting on behalf of NASA:

- A.) Makes any warranty or representation, expressed or implied, with respect to the accuracy, completeness, or usefulness of the information contained in this report, or that the use of any information, apparatus, method or process disclosed in this report may not infringe privately owned rights, or
- B.) Assumes any liabilities with respect to the use of, or for damages resulting from the use of any information, apparatus, method or process disclosed in this report.

As used above, "person acting on behalf of NASA" includes any employee or contractor of NASA, or employee of such contractor, to the extent that such employee or contractor of NASA, or employee of such contractor prepares, disseminates, or provides access to, any information pursuant to his employment or contract with NASA, or his employment with such contractor.

Requests for copies of this report should be referred to:

National Aeronautics and Space Administration
Office of Scientific and Technical Information
Attention: AFSS-A
Washington, D. C. 20546

NASA CR-54961
AGC 8800-64

TECHNOLOGY REPORT

SUMMARY OF MATERIALS TECHNOLOGY
OF M-1 ENGINE

Prepared for

NATIONAL AERONAUTICS AND SPACE ADMINISTRATION

22 July 1966

CONTRACT NAS 3-2555

Prepared by:

AEROJET-GENERAL CORPORATION
LIQUID ROCKET OPERATIONS
SACRAMENTO, CALIFORNIA

AUTHOR: G. R. Janser

APPROVED: V. Frick
M-1 Materials Engineering

Technical Management:

NASA LEWIS RESEARCH CENTER
CLEVELAND, OHIO

TECHNICAL MANAGER: J. M. Kazaroff

APPROVED: W. W. Wilcox
M-1 Project Manager

ABSTRACT

3 3977

This report is a compilation of Aerojet-General Materials Engineering tasks of limited scope performed in support of the M-1 Engine Program. These tasks include the determination of cryogenic properties of selected materials, welding of AISI 347 stainless steel to Inconel 718, fabrication properties of Rigimesh, and cryogenic property evaluations of wrought and cast 5Al-2.5-Sn-ELI titanium for pump inducers. The major materials studies are reported separately and are referenced.

TABLE OF CONTENTS

	<u>Page</u>
I. <u>SUMMARY</u>	1
II. <u>INTRODUCTION</u>	1
III. <u>THERMAL EXPANSION OF SELECTED TURBOPUMP MATERIALS</u>	1
IV. <u>MECHANICAL PROPERTIES OF AISI 9310 LOW-ALLOY STEEL WELDS</u>	1
V. <u>LOW-TEMPERATURE PROPERTIES OF 18% NICKEL MARAGING STEEL</u>	3
VI. <u>THRUST CHAMBER ASSEMBLY JACKET FIT-UP</u>	11
A. FIT-UP STUDY RESULTS	11
B. ADHESIVE MATERIALS STUDY RESULTS	12
C. CONCLUSIONS	14
VII. <u>WELDING OF AISI 347 STAINLESS STEEL TO INCONEL 718</u>	22
VIII. <u>EVALUATION OF HEAT-REFLECTIVE COATINGS FOR THRUST CHAMBER SUPPORTS</u>	22
A. LABORATORY INVESTIGATION	27
B. PRODUCT LITERATURE SURVEY	31
C. CONCLUSIONS	31
D. RECOMMENDATIONS	31
IX. <u>TORSIONAL PROPERTIES OF INCONEL X-750</u>	32
X. <u>DIMENSIONAL STABILITY OF AISI 440C STAINLESS STEEL</u>	34
A. INVESTIGATION RESULTS	34
B. CONCLUSIONS	38

TABLE OF CONTENTS (Cont'd)

	<u>Page</u>
C. RECOMMENDATION	38
XI. <u>RIGIMESH MECHANICAL PROPERTIES AND FABRICATION CHARACTERISTICS</u>	38
A. MECHANICAL AND PHYSICAL PROPERTIES	39
B. DETERMINATION OF PROCESS CHARACTERISTICS	39
XII. <u>LARGE TITANIUM 5Al-2.5 Sn-ELI PUMP INDUCER FORGING EVALUATION</u>	51
A. PROCEDURE	52
B. RESULTS	52
C. CONCLUSIONS	55
D. RECOMMENDATION	55
XIII. <u>CAST TITANIUM 5Al-2.5 Sn-ELI PUMP INDUCER EVALUATION</u>	55
A. PROCEDURE	58
B. RESULTS	61
C. CONCLUSIONS	69
D. RECOMMENDATIONS	75

BIBLIOGRAPHY

LIST OF TABLES

<u>Table</u>	<u>Title</u>	<u>Page</u>
I.	Tensile Properties of AISI 9310 Steel Parent Metal	4
II.	Tensile Properties of AISI 9310 Steel Welds Made with 8018-C2 (ASTM-4-316-58T) Electrodes	5
III.	Tensile Properties of 0.090-in. 18% Nickel Maraging Steel Sheet Heat Treated 1 hr. @ 1500°F A.C., Aged 3 hrs @ 900°F A.C.	6
IV.	Tensile Properties of 18% Nickel Maraging Steel Forging Solution-Annealed and Aged	8
V.	Coefficient of Expansion for 18% Nickel Maraging Steel	9
VI.	Shear Strength of Epoxy Adhesives	13
VII.	Shear Strength of X-Epon 99-105-1 Epoxy Adhesive at Room Temperature and -320°F	15
VIII.	Compressive Strength of Epoxy Adhesives	16
IX.	Tensile Properties of Epoxy Adhesives at Room Temperature and -320°F	17
X.	Flow Characteristics of X-Epon 99-105-1 Epoxy Adhesive	18
XI.	Coefficient of Thermal Expansion from -320°F to Room Temperature for Machined Epoxy Specimens	19
XII.	Coefficient of Thermal Expansion from -320°F to Room Temperature for Molded Epoxy Specimens	20
XIII.	Room Temperature Tensile Properties of Inconel 718-347 Stainless Steel Weldments	23
XIV.	Typical Properties of 347 Stainless Steel and Inconel 718 Alloys	26
XV.	Thermal Stability of Heat Reflective Coatings from Temperature of -320°F to 2000°F	28
XVI.	Torsional Properties of Inconel X-750 Alloy (Aged -1300°F/ 20 Hr)	33

LIST OF TABLES (Cont'd)

<u>Table</u>	<u>Title</u>	<u>Page</u>
XVII.	Tensile Properties of Inconel X-750 Alloy (Aged -1300°F /20 hr)	35
XVIII.	Dimensions of AISI 440C Stainless Steel Roller Bearings After Soaking at Various Cryogenic Temperatures	36
XIX.	Retained Austenite Vs. Temperature for Heat Treated AISI 440C Stainless Steel Roller Bearings	37
XX.	Thermal Expansion of Rigimesh	40
XXI.	Mechanical Properties of 0.125-in. Rigimesh Sheet	41
XXII.	Mechanical Properties of TIG and EB Welded Rigimesh	45
XXIII.	Tensile Properties of Alpha Titanium Alloy (Ti-5Al-2.5Sn-ELI) Fuel Inducer Forging Blank	53
XXIV.	Yield Strength (0.2% Offset)-to-Density Ratio of Pump Inducer Materials	54
XXV.	Chemical Analysis of Ti-5Al-2.5Sn-ELI Forging	56
XXVI.	Radiographic Inspection Data for Pump Inducer Casting (Vane Section)	62
XXVII.	Mechanical Properties of 5Al-2.5Sn-ELI Titanium Alloy Pump Inducer Casting (Vane Section)	63
XXVIII.	Chemical Composition of Experimental M-1 Fuel Pump Impeller Casting of Titanium Alloy 5Al-2.5Sn-ELI	70

LIST OF FIGURES

<u>Figure</u>	<u>Title</u>	<u>Page</u>
1.	Expansion Vs. Temperature for M-1 Turbopump Assembly Materials	2
2.	Tensile Test Results on 18% Nickel Maraging Steel Sheet (0.090-in.)	10
3.	Linear Thermal Expansion Coefficients of Epoxy Materials	21
4.	Thermal Stability of Heat-Reflective Coatings	30
5.	Test Bars Showing Typical Fracture of Rigimesh	42
6.	Section of Porous Metal Across Woof, Polished, and Etched	43
7.	Butt Weld, Woof-to-Woof, of Rigimesh	46
8.	EB Butt Weld, Warp-to-Sheet of Rigimesh	46
9.	TIG Butt Weld, Woof-to-Sheet, of Rigimesh	46
10.	Macrograph of AISI 347 Stainless Steel Spacer Welded to AISI 347 Stainless Rigimesh Sheet by the Electron-Beam Process	47
11.	Photomicrograph of AISI 347 Stainless Steel Sheet Welded to AISI 347 Stainless Steel Rigimesh Sheet by the Electron-Beam Process (24X)	48
12.	Photomicrograph of Electron-Beam Weld in Rigimesh Showing Cracking at a Nugget-Pore Intersection (100X)	49
13.	Braze Alloy Penetration into Porous Metal Sheet (5X)	50
14.	Microstructure of Titanium Alloy 5Al-2.5Sn-ELI Pump Inducer Forging	57
15.	Simulated Fuel Pump Inducer Casting of Titanium Alloy 5Al-2.5Sn-ELI	59
16.	Simulated Fuel Pump Inducer Casting of Titanium Alloy 5Al-2.5Sn-ELI Showing Weld Repair Area	60
17.	Mechanical Properties of Cast Ti-5Al-2.5Sn-ELI and 7079-T652 Aluminum Pump Inducers	65

LIST OF FIGURES (Cont'd)

<u>Figure</u>	<u>Title</u>	<u>Page</u>
18.	Notch Tensile and Notch-Yield Ratios of Cast Ti-5Al-2.5 Sn-ELI and 7079-T652 Aluminum Pump Inducers	66
19.	0.2% Yield Strength-Density Ratio of Cast Ti-5Al-2.5 Sn-ELI and 7079-T652 Aluminum Pump Inducers	67
20.	Macrostructure of Vane and Repair Weld in Vane	68
21.	Microstructure of Vane Section	71
22.	Titanium Alloy-Graphite Mold Reaction Zone	71
23.	Cracked Welds in Dye-Penetrant Condition	72
24.	Cracked Weld in Macro-Etched Condition	73
25.	Cracked Weld in Dye-Penetrant Condition	73
26.	Sound Weld in Dye-Penetrant Condition	74

I. SUMMARY

Numerous tasks were performed by Aerojet-General Materials Engineering in support of the design and fabrication of the M-1, a 1.5 million-lb-thrust liquid hydrogen/liquid oxygen engine. The major studies concerning the application of extremely large 7079 aluminum forgings, use of Inconel 718, development of alloys for vacuum furnace brazing, and induction processed separable tubular connectors, were reported individually. This report is a compilation of other tasks considered significant but of limited scope. The limitation resulted from a redirection of the design and/or fabrication effort; however, the data generated are considered useful for determining future engine applications.

II. INTRODUCTION

Major studies performed by the Aerojet-General Materials Engineering organization in support of the M-1 Program have been reported in separate NASA-Contractor type reports (1)(2)(3)(4). Numerous other tasks of significant but limited scope were also performed. It is this latter work that is reported herein.

III. THERMAL EXPANSION OF SELECTED TURBOPUMP MATERIALS

The purpose of this investigation was to establish expansion-versus-temperature curves for turbopump materials located in critical fit-up areas. These data were required for design purposes so as to provide proper assembly fits during operation at cryogenic temperatures after pump chill-down as well as for ease of disassembly at ambient temperatures.

The expansion curves for Invar 36, AISI 440C stainless steel, Rene' 41, and Inconel 718 in the temperature range from ambient to -423°F are shown in Figure No. 1. All materials, with the exception of Invar 36, had been heat treated. The expansion curves represent the results of literature surveys and laboratory tests conducted by Aerojet-General as well as two independent laboratories.

IV. MECHANICAL PROPERTIES OF AISI 9310 LOW-ALLOY STEEL WELDS

The AISI 9310 low-alloy steel was selected as the material for the initial engine support struts because of its relatively low cost as well as adequate

- (1) Inouye, F. T., Properties of Large 7079 Aluminum Forgings, Aerojet-General Report No. 8800-20, 9 February 1966
- (2) Inouye, F. T., Hunt, V., Janser, G. R., and Frick, V., Summary of Experience Using Inconel 718 on M-1 Engine, Aerojet-General Report No. 8800-57, 30 December 1965
- (3) Gustafson, K. L., Development and Evaluation of Braze Alloys for Vacuum Furnace Brazing, Aerojet-General Report No. 8800-26, 5 November 1965
- (4) Hunt, V., Induction Processed Separable Tubular Brazed Connectors, Aerojet-General Report No. 8800-24, 5 November 1965

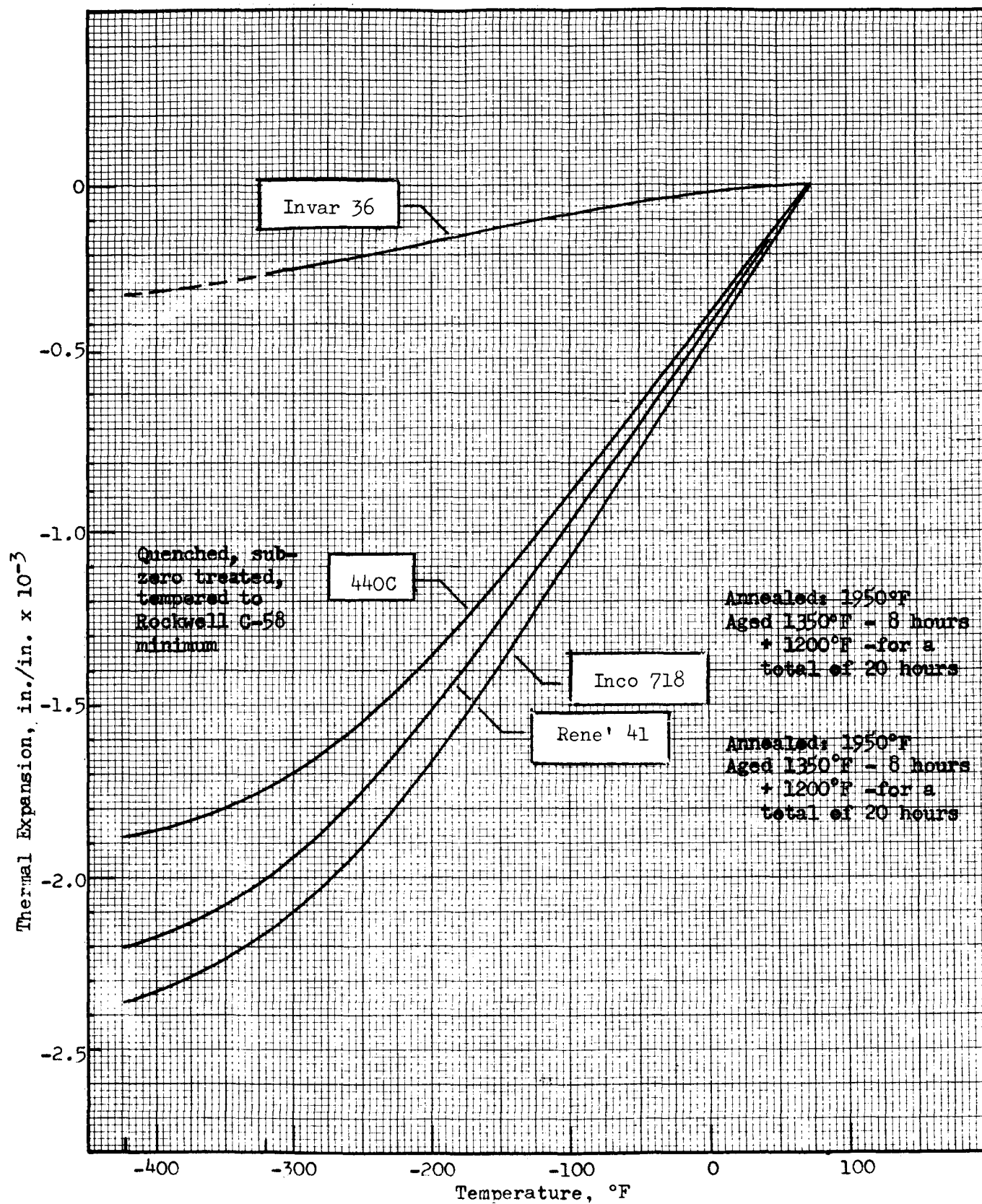


Figure 1

Expansion Vs. Temperature for M-1 Turbopump Assembly Materials

strength and low temperature ductility for the selected application (Table I). However, AISI 9310 steel was not readily available in wire form, and little or no information existed about filler rods that would provide the required low temperature toughness. What information was available indicated that the Class E, 8018C-2 (ASTM - A 316-58T) electrode might be satisfactory to a temperature of -200°F.

An investigation was initiated to evaluate AISI 9310 weldments made with 8018 C-2, 200-ksi grade 18% nickel maraging steel, and 9 nickel-4 cobalt alloy filler rods. Notched and unnotched tensile tests and Charpy V-notch impact tests were scheduled at room temperature, -100°F, and -320°F. This work was terminated after the completion of tensile testing of the weldments made with the 8018 C-2 wire. Results of these tests (Table II) indicate that the 8018 C-2 wire would be satisfactory for the application.

V. LOW TEMPERATURE PROPERTIES OF 18% NICKEL MARAGING STEEL

A 250 ksi grade 18% nickel maraging steel was evaluated for applications where coatings could be used to provide corrosion resistance as well as where it was needed to provide strength or weight savings.

This material was considered for the support struts, helium pressure vessel, and propellant line bellows joint support bearings. Initial stress analysis for the latter application indicated that the 250-ksi yield strength was required.

Ambient and low temperature testing was scheduled with an 0.090-in. thick sheet (air and vacuum melted) that was available on-plant at that time. Sheet metal 0.060-in., 0.125-in., and 0.250-in. thick at both 200 ksi and 250 ksi yield strength levels in the air- and vacuum-melted conditions were ordered. However, this material was not procured because of budgetary limitations. Support bearing forgings were also obtained for evaluation. These bearings are of a ball and socket configuration. They support the axial load in the propellant line bellows joint.

Subsize flat notched and unnotched tensile specimens were machined from the 0.090-in. gage sheet 18% nickel maraging steel. One set of specimens was taken from the air-melted sheet and one set from the vacuum-arc-remelted sheet. The specimens were solution annealed for one hour at 1500°F, aged three hours at 900°F, and tensile tested at room temperature, -100°F and -420°F. The subsize, 1/4-in. x 1-in. gage specimens were required because testing a full-size specimen at -420°F would have exceeded the capacity of the tensile machine. A summary of test results are listed in Table III and shown graphically in Figure No. 2.

Three R-4 tensile specimens were machined from the longitudinal direction and three from the transverse direction (see Table IV for specimen location) in each of the two 18% nickel maraging steel bearings. These were then tested at room temperature, -320°F, and -423°F (Table IV).

An expansion-versus-temperature curve was determined for the 250-ksi yield strength material at temperatures ranging from ambient to -320°F. The results are listed in Table V.

TABLE I

TENSILE PROPERTIES OF AISI 9310 STEEL PARENT MATERIAL*
ON SMOOTH AND NOTCHED SPECIMENS AT VARIOUS TEMPERATURES

<u>Specimen No.</u>	<u>Test Temp.</u>	<u>Ultimate (ksi)</u>	<u>Yield 0.2% Offset</u>	<u>Elongation (%/in.)</u>	<u>Reduction of Area(%)</u>
P-1	RT	183.7	150.7	16.5	66.8
P-2	RT	183.3	153.1	16.0	62.4
P-3	RT	<u>182.9</u>	<u>150.0</u>	<u>17.0</u>	<u>66.2</u>
	Averages	183.3	151.6	16.5	65.0
P-4	-100°F	195.3	162.5	18.0	67.5
P-5	-100°F	195.2	160.4	19.5	65.7
P-6	-100°F	<u>194.1</u>	<u>159.8</u>	<u>19.0</u>	<u>68.2</u>
	Averages	194.8	160.9	19.0	67.0
P-7	-320°F	233.0	205.8	18.5	55.9
P-8	-320°F	231.5	199.0	22.0	57.0
P-9	-320°F	<u>231.6</u>	<u>199.2</u>	<u>19.0</u>	<u>60.7</u>
	Averages	232.0	201.3	20.0	57.0
VP1	RT	258.7	Kt = 7.2	At Room Temperature the notch to smooth tensile ratio is 1.42	
VP2	RT	259.3	Kt = 7.1		
VP3	RT	<u>258.1</u>	Kt = 7.7		
	Average	258.7			
VP4	-100°F	276.9	Kt = 6.8	At -100°F the notch to smooth tensile ratio is 1.37	
VP5	-100°F	268.5	Kt = 6.7		
VP6	-100°F	<u>258.8</u>	Kt = 5.0		
	Average	268.1			
VP7	-320°F	305.0	Kt = 5.6	At -320°F the notch to smooth tensile ratio is 1.28	
VP8	-320°F	307.5	Kt = 5.8		
VP9	-320°F	<u>290.3</u>	Kt = 5.0		
	Average	300.9			

P - Parent Material Smooth Specimen

V - Notched Specimen

* Heat Treatment: Austenitized 1500°F, O.Q., tempered at 350°F for 1 hour.

TABLE II

MECHANICAL PROPERTIES OF AISI 9310 STEEL WELDS*
MADE WITH 8018-C2 (ASTM-A-316-58T) ELECTRODES

<u>Specimen Number</u>	<u>Test Temp.</u>	<u>Ultimate Strength (ksi)</u>	<u>0.2% Offset Yield Strength (ksi)</u>	<u>Elongation % (4D)</u>	<u>Reduction of Area(%)</u>	<u>Remarks</u>
W1**	RT	120.6	91.2	5.5	25.3	Failure occurred in welds
W2	RT	107.9	79.8	13.5	63.5	
W3	RT	<u>103.1</u>	<u>73.7</u>	<u>15.0</u>	<u>61.9</u>	
Averages		110.5	81.5	11.4	50.0	
W4	-100°F	120.6	79.4	10.0	47.3	Failure occurred in welds
W5	-100°F	128.2	97.4	11.5	52.5	
W6	-100°F	<u>123.0</u>	<u>83.0</u>	<u>16.0</u>	<u>61.7</u>	
Averages		123.9	86.6	12.5	53.8	
W7	-320°F	172.1	141.0	4.5	16.2	Failure occurred in welds
W8	-320°F	167.1	140.5	5.5	22.1	
W9	-320°F	<u>169.9</u>	<u>137.9</u>	<u>5.5</u>	<u>20.2</u>	
Averages		169.7	139.8	5.2	19.5	
VW**1	RT	129.3	Kt = 4.5	at room temperature the notch-to-smooth tensile ratio is 1.18		
VW2	RT	132.3	Kt = 4.4			
VW3	RT	<u>137.7</u>	Kt = 5.7			
Average		133.1				
VW4	-100°F	135.8	Kt = 3.4	at -100°F the notch-to-smooth tensile ratio is 1.09		
VW5	-100°F	132.5	Kt = 5.8			
VW6	-100°F	<u>137.6</u>	Kt = 3.7			
Average		135.3				
VW7	-320°F	155.0	Kt = 4.4	at -320°F the notch-to-smooth tensile ratio is .96		
VW8	-320°F	173.2	Kt = 7.1			
VW9	-320°F	<u>159.2</u>	Kt = 6.8			
Average		162.4				

* Heat treatment: Austenitized 1500°F, O.Q., tempered at 350°F 1 hour.

** W - smooth test specimens

VW - notched test specimens

TABLE III

TENSILE PROPERTIES OF 0.090-IN. 18% NI MARAGING STEEL SHEET
HEAT TREATED 1 HR @ 1500°F A.C., AGED 3 HRS @ 900°F A.C.

A. SMOOTH TENSILE SPECIMENS

Specimen No.	Orientation	Melting Procedure	Test Temp °F	UTS ksi	Yield Str. ksi	Elongation %/4X Width	Hardness R _C
LA-1	Long.	Air	R.T.	254	245	4.5	48.5
LA-2	Long.	Air	R.T.	256	250	4.5	48.5
TA-1	Trans	Air	R.T.	249	244	4.5	48.0
TA-2	Trans	Air	R.T.	248	245	4.5	48.0
LV-1	Long.	Vacuum	R.T.	247	243	4.5	49.0
LV-2	Long.	Vacuum	R.T.	249	244	4.0	49.0
TV-1	Trans	Vacuum	R.T.	250	244	4.5	49.0
TV-2	Trans	Vacuum	R.T.	251	245	4.5	49.0
LA-1	Long.	Air	-320	325	309	7.0	
TA-1	Trans	Air	-320	316	302	7.0	
LV-1	Long.	Vacuum	-320	320	306	7.0	
TV-1	Trans	Vacuum	-320	318	298	7.0	
LV-1	Long.	Vacuum	-420	350	---	2.0	
LV-2	Long.	Vacuum	-420	362	350	2.5	
TV-1	Trans	Vacuum	-420	362	347	3.0	
TV-2	Trans	Vacuum	-420	368	354	2.5	
LA-1	Long.	Air	-420	356	344	3.0	
LA-2	Long.	Air	-420	329	---	3.0	
TA-1	Trans	Air	-420	360	355	3.0	

TABLE III (cont.)

B. NOTCHED TENSILE SPECIMENS

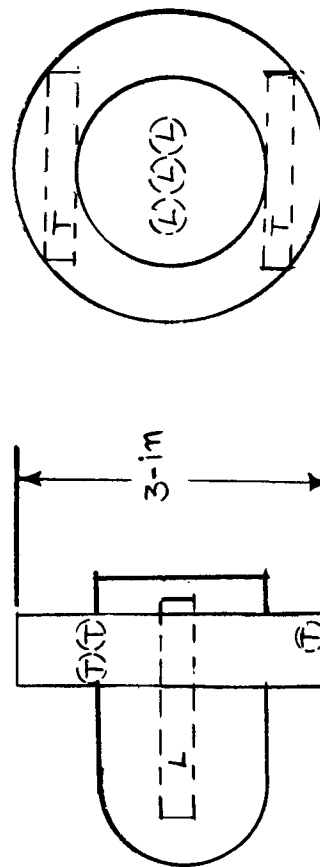
Specimen No.	Orientation	Melting Procedure	Test Temp °F	Notched Tensile Str. ksi	K _t	Notched-Unnotched Ratio	Hardness R _c
LA-1	Long.	Air	R.T.	277	9-11	1.07	47.5
LA-2	Long.	Air	R.T.	268	9-11		47.5
TA-1	Trans	Air	R.T.	269	9-11	1.08	48.0
TA-2	Trans	Air	R.T.	267	9-11		48.0
LV-1	Long.	Vacuum	R.T.	264	9-11	1.05	47.5
LV-2	Long.	Vacuum	R.T.	258	9-11		47.5
TV-1	Trans	Vacuum	R.T.	268	9-11	1.06	48.5
TV-2	Trans	Vacuum	R.T.	266	9-11		48.5
LA-1	Long.	Air	-320	282	9-11	0.90	
LA-2	Long.	Air	-320	299	9-11		
TA-1	Trans	Air	-320	311	9-11	0.96	
TA-2	Trans	Air	-320	293	9-11		
LV-1	Long.	Vacuum	-320	304	9-11	0.94	
LV-2	Long.	Vacuum	-320	297	9-11		
TV-1	Trans	Vacuum	-320	295	9-11	0.96	
TV-2	Trans	Vacuum	-320	273	9-11		
LV-1	Long.	Vacuum	-420	325	5.5-6.5	0.89	
LV-2	Long.	Vacuum	-420	330	5.5-6.5	0.89	
LV-3	Long.	Vacuum	-420	312	5.5-6.5	0.89	
TV-1	Trans	Vacuum	-420	294	5.5-6.5	0.89	
TV-2	Trans	Vacuum	-420	329	5.5-6.5	0.89	
TV-3	Trans	Vacuum	-420	347	5.5-6.5	0.89	
LA-1	Long.	Air	-420	349	5.5-6.5	0.90	
LA-2	Long.	Air	-420	307	5.5-6.5	0.90	
LA-3	Long.	Air	-420	328	5.5-6.5	0.90	
TA-1	Trans	Air	-420	337	5.5-6.5	0.90	
TA-2	Trans	Air	-420	323	5.5-6.5	0.90	
TA-3	Trans	Air	-420	303	5.5-6.5	0.90	

TABLE IV

TENSILE PROPERTIES OF 18% NICKEL MARAGING STEEL FORGING
SOLUTION-ANNEALED AND AGED

Test Temp (°F)	Orientation	Ultimate Tensile Strength, (ksi)	0.2% Offset		Reduction in Area (%)	Hardness, Rc
			Yield Strength, (ksi)	% Elong. in 4D		
1. R.T.	Longitudinal	290.2	273.5	9.4	46.6	54
2. R.T.	Longitudinal	283.5	270.0	7.0	29.6	52
3. R.T.	Transverse	286.6	273.6	6.3	24.4	52
4. R.T.	Transverse	286.3	272.1	6.3	24.5	52
AGC Specification Requirements		--	250.0 min.	2.0 min.	40-Longitudinal 32-Transverse	--
1. -320	Longitudinal	362.8	294.1	6.3	28.9	--
2. -320	Longitudinal	362.2	288.6	7.0	33.8	--
3. -320	Transverse	356.9	286.8	3.9	15.7	--
4. -320	Transverse	356.3	281.6	3.9	9.7	--
1. -423	Longitudinal	377.5	375.0*	DUCTILITY TOO LOW TO MEASURE		--
2. -423	Longitudinal	364.5	362.0*			--
3. -423	Transverse	373.0	368.0*			--
4. -423	Transverse	388.0	378.5*			--

* 0.1% Offset Yield Strength



SPECIMEN LOCATION

TABLE V

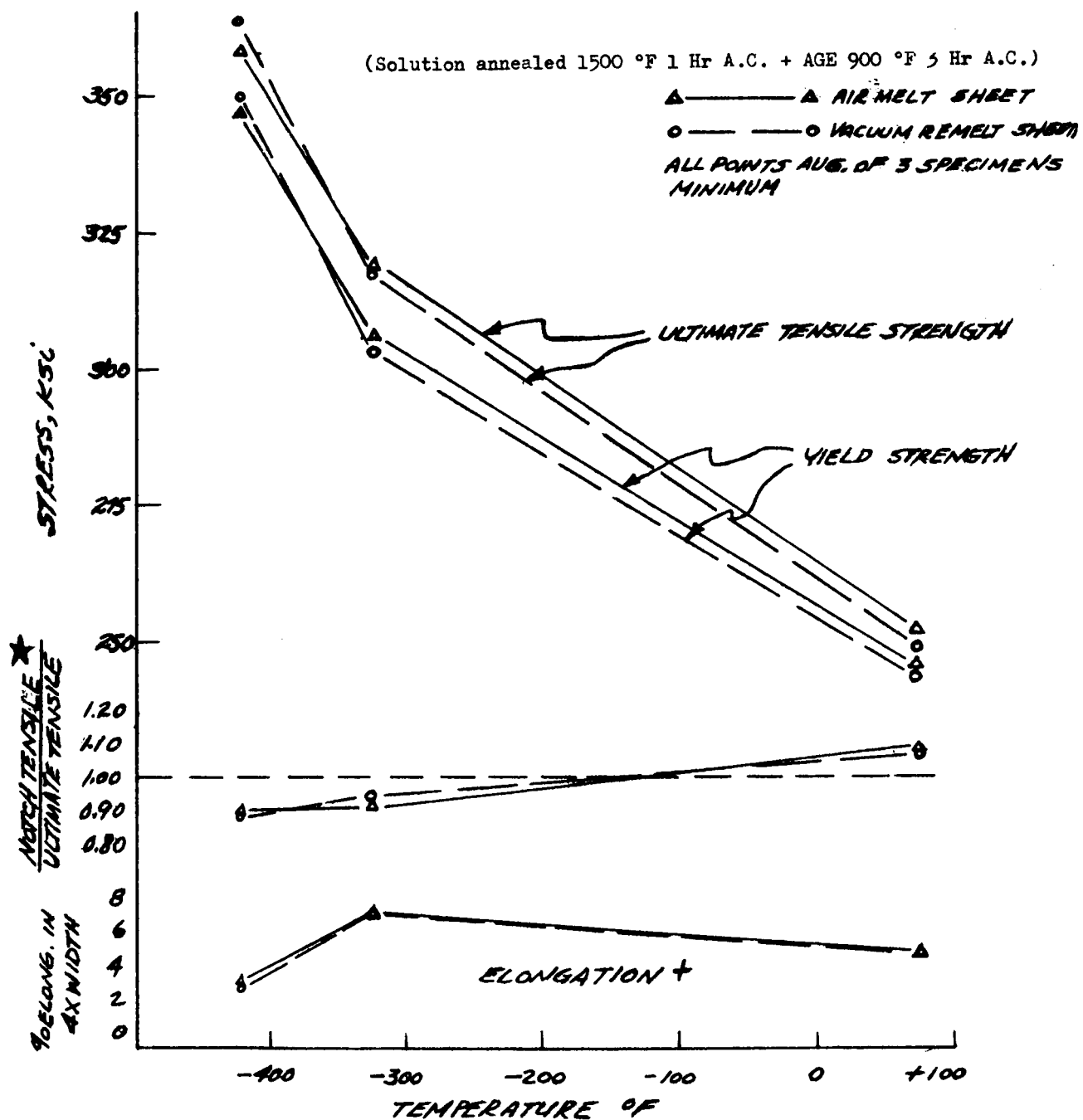
COEFFICIENT OF EXPANSION FOR 18% NICKEL MARAGING STEEL

Solution-Annealed Condition

68°F to 0°F	5.56×10^{-6} in./in./°F
68°F to -100°F	5.42×10^{-6} in./in./°F
68°F to -200°F	4.94×10^{-6} in./in./°F
68°F to -300°F	4.63×10^{-6} in./in./°F
68°F to -316°F	4.53×10^{-6} in./in./°F

Solution-Annealed and Aged Condition

68°F to 0°F	4.71×10^{-6} in./in./°F
68°F to -100°F	4.68×10^{-6} in./in./°F
68°F to -200°F	4.55×10^{-6} in./in./°F
68°F to -300°F	4.31×10^{-6} in./in./°F
68°F to -316°F	4.30×10^{-6} in./in./°F



★ $K_t = 9-11$ for room temp & -320 °F tests.
 $= 5.5-6.5$ for -420 °F test

+ Room temperature elongation measured on standard $\frac{1}{2}$ in. x 2 in. Gage.
 -320 °F & -420 °F elongation measured on substandard $\frac{1}{4}$ in. x 1 in. Gage.

Figure 2

Tensile Test Results on 18% Nickel Maraging Steel Sheet (0.090-in.)

The 0.090-in. sheet shows a significant rise in tensile and yield strength with decreasing temperature with no appreciable strength difference between the air-melted and vacuum-melted materials. The notch toughness and ductility, as represented by the notch-unnotched tensile ratios and elongation values, indicate that the material possesses adequate ductility to -420°F in this thickness. As with strength values, the notch toughness and elongation values are nearly equivalent for the air-melted and vacuum-melted material.

The ductility of the 250-ksi yield strength forgings was found to be satisfactory at room temperature and -320°F, but is inadequate at -420°F.

This limited testing indicates that the 250-ksi yield strength, 18% nickel maraging in thin sheet and moderate size forgings shows promise for use as structural members where high strength and good notch toughness are required at cryogenic temperatures. However, additional research is required to establish the interrelated effects of strength grade, vacuum remelting, rolling or forging direction, and thickness on the properties of 18% nickel maraging steel.

VI. THRUST CHAMBER ASSEMBLY JACKET FIT-UP

The purpose of this investigation was to evaluate materials to fill the space between the engine thrust chamber and its reinforcing jacket. The filler material was required to provide even distribution of the load transmitted to the jacket from the tubular chamber assembly during engine firing. A spacing was also needed to accommodate a foil or film that would be used to prevent the selected gap-filling material from sealing the longitudinal indentations between tubes. The axial depressions between the tubes have been specified as required paths for overboard dissipation of hydrogen in the event of tube leakage.

A. FIT-UP STUDY RESULTS

A study of the anticipated fit-up problem revealed that the selected gap-filling material must have the following capabilities:

1. Flexibility to compensate for deformation of the metal components during cool down.
2. Yield strengths greater than the involved structural stresses, particularly at cryogenic temperatures.
3. Thermal expansion values approaching those of the thrust chamber jacket material.
4. Insensitivity to detonation in the presence of liquid air or oxygen.
5. Ability to bond securely to the thrust chamber jacket, fill small gaps, and be easily applied.

Flexible epoxy resin systems most closely meet the application requirements. These systems have a relatively low glass-transition temperature, high-strength values, and moderate bond strength at low temperatures. Their thermal expansion values approximate those for the 300 series stainless steels when reinforced with aluminum powder or glass fiber. However, epoxy composites are moderately sensitive to impact in the presence of oxygen, but the above-mentioned foil or film would bond to the composite and protect it against liquid air or oxygen contact.

The viscosity of an epoxy system can be varied considerably by adding a thixotropic agent. Thus, depending upon its original minimum viscosity, methods for applying the material can vary from casting or injecting to troweling. If ports can be provided in the thrust chamber jacket and the minimum viscosity of a selected composite permits, the composite may be injected between the jacket and the foil or film placed on the outside diameter of the tube bundle. If the minimum viscosity of the selected composite approaches a paste, then the material might be troweled onto the inner surface of the jacket. The jacket would then be installed and excess material allowed to extrude. Curing of such a resin system could range from room temperature to 350°F. During application of the composite, the foil or film functions as a mold release for the thrust chamber tube bundle.

B. ADHESIVE MATERIALS STUDY RESULTS

Four adhesive materials (Shell Chemical Co.) were investigated.

1. X-Epon 99-105-1

This is a semi-flexible, aluminum-filled epoxy resin system. It is a paste-like material, readily trowelable, and may be easily applied.

2. X-Epon 99-105-2

This is a flexible, aluminum-filled epoxy resin system. It will flow and can be cast.

3. X-Epon 99-105-3

This is a semi-rigid, aluminum-filled epoxy resin system. It will not flow and has a consistency between trowelable and castable.

4. Epon 901/B-3 and Epon 901/B-1

This is a rigid, filled epoxy resin system. It is thixotropic with a consistency of butter. Curing agent B-3 provides somewhat better high temperature strength than curing Agent B-1.

Results of the initial investigation to determine lap shear strengths of the four adhesives at room temperature and -320° are given in Table VI. The three experimental Epon adhesives 99-105-1, -2, and -3, were cured for one-half hour at 140°F plus one-half hour at 300°F, as recommended by the manufacturer; whereas the Epon 901/B-3 adhesive was cured for one-half hour at 240°F

TABLE VI
SHEAR STRENGTH OF EPOXY ADHESIVES

A.	<u>Adhesive Material</u>	Avg. Lap-Shear Strength at Room Temp. (68°F)	<u>Failure Type</u>
	X-Epon 99-105-1	1440 psi	cohesive
	X-Epon 99-105-2	1240 psi	adhesive
	X-Epon 99-105-3	990 psi	adhesive
	Epon 901/B-3	880 psi	adhesive

B.	<u>Adhesive Material</u>	Avg. Lap-Shear Strength at IN ₂ Temp (-320°F) ²	<u>Failure Type</u>
	X-Epon 99-105-1	2265 psi	cohesive
	X-Epon 99-105-2	1400 psi	adhesive
	X-Epon 99-105-3	1580 psi	adhesive
	Epon 901/B-3	790 psi	adhesive

Lap-shear strength of aluminum-to-aluminum bonded specimens (1-in. overlap; 1-in.² bond area). Five specimens were tested at each temperature in accordance with ASTM-D-1002.

plus one and one-half hours at 350°F. The X-Epon 99-105-1 adhesive shows a cohesive failure of the bond at both room temperature and -320°F; whereas, the other materials failed in adhesion. Lap shear strength was determined during a subsequent cure cycle and is shown in Table VII. The compressive strengths of the four adhesives were also determined and these are given in Table VIII.

The three experimental Epon adhesives (99-105-1, -2, and -3) were cured one-half hour at 140°F plus one-half hour at 300°F; whereas, the Epon 901/B-3 adhesive was cured one-half hour at 240°F plus one and one-half hours at 350°F. For a flexible system, X-Epon 99-105-1 showed the best compressive properties at -320°F with relatively similar compressive strain values at failure for both 68°F and -320°F test conditions. Examination of the ruptured compressive strength specimens revealed that the X-Epon 99-105-1 material was the most homogenous in structure and is recommended as the best adhesive. The X-Epon 99-105-2 and -3 specimens showed poor resin distribution and are not recommended for adhesive fill materials. The Epon 901/B-3 specimens showed excessive voids and would require an improved curing process to be acceptable for the stated application.

Comparative tensile properties of Epon 901/B-1 and X-Epon 99-105-1 are given in Table IX. An average tensile strength of 1565 psi at room temperature and 11,160 psi at -320°F was measured for X-Epon 99-105-1, with elongation of 5% to 14% and 1% to 5% recorded at the respective temperatures.

Flow characteristics of X-Epon 99-105-1 are presented in Table X. Results indicate that the adhesive may be applied at a thickness of 0.125-in. on a vertical surface without excessive flow during cure.

Coefficient of thermal expansion data from -320°F to room temperature are given in Tables XI and XII. A graphical illustration of this data is shown in Figure No. 3. A mean coefficient ranging from 22×10^{-6} in./in./°F (-320°F to room temperature) to 40×10^{-6} in./in./°F (0°F to room temperature) was measured for the X-Epon 99-105-1 adhesive.

C. CONCLUSIONS

1. The experimental Epon 99-105-1 (a 70% aluminum-filled, flexible epoxy system) developed by Shell Chemical Co. for this investigation is considerably more ductile than the Epon 901 adhesives at cryogenic temperatures.
2. Thermal expansion data from -320°F to room temperature indicate that the more rigid Epon 901 adhesives have lower expansion rates than the flexible X-Epon 99-105 system.
3. The initial shear and compressive strength data are for aluminum-to-aluminum bonded specimens. Further shear testing of Inconel 718-to-Inconel 718 specimens bonded with Epon 99-105-1 adhesive shows the shear-strength advantage of the higher temperature (300°F) cure.

TABLE VII
SHEAR STRENGTH OF X-EPON 99-105-1 EPOXY ADHESIVE
AT ROOM TEMPERATURE AND -320°F

A.	<u>Adhesive Cure</u>	<u>Shear Strength at 77°F (psi)</u>	<u>Type Failure</u>
	24 hr at 120°F	1205	cohesive
		<u>1120</u>	adhesive
		1162 (avg.)	
	30 min. at 140°F	1130	cohesive
	plus ½ hr at 300°F	<u>1225</u>	cohesive
		1177 (avg.)	
B.	<u>Adhesive Cure</u>	<u>Shear Strength at -320°F (psi)</u>	<u>Type Failure</u>
	24 hr at 120°F	1315	adhesive
		<u>1520</u>	adhesive
		1417 (avg.)	
	30 min. at 140°F	2475	adhesive
	plus ½ hr at 300°F	<u>2470</u>	adhesive
		2472 (avg.)	

Lap-shear strength of Inconel 718-to-Inconel 718 bonded specimens. Two cured specimens were tested at each temperature in accordance with ASTM-D-1002. (All metal coupons were surface-abraded with 180 grit emery cloth and wiped with trichlorethylene prior to bonding in accordance with MSFC 10M01572.)

TABLE VIII
COMPRESSIVE STRENGTH OF EPOXY ADHESIVES

A.	<u>Adhesive Material</u>	<u>Average Compressive Strength at Room Temperature (68°F)</u>	<u>Percent Compressive Strain at Failure</u>
	X-Epon 99-105-1	8,700 psi	44%
	X-Epon 99-105-2	21,000 psi	62%
	X-Epon 99-105-3	3,400 psi	40%
	Epon 901/B-3	13,800 psi	13%

B.	<u>Adhesive Material</u>	<u>Average Compressive Strength at LN₂ Temperature (-320°F)</u>	<u>Percent Compressive Strain at Failure</u>
	X-Epon 99-105-1	63,000 psi	32%
	X-Epon 99-105-2	51,000 psi	16%
	X-Epon 99-105-3	42,700 psi	12%
	Epon 901/B-3	39,200 psi	16%

Compressive strength and % strain at failure in accordance with ASTM-D-695. Three X-Epon adhesive materials (1-in. long x 0.5 x 0.5-in. - Specimens 0.25 in.² compressive area) Epon 901/B-3 (1-in. long x 0.5-in. diameter - Specimens 0.19 in.² compressive area).

TABLE IX
TENSILE PROPERTIES* OF EPOXY ADHESIVES
AT ROOM TEMPERATURE AND -320°F

A.	<u>Adhesive</u>	Average Tensile	Elongation
		Strength at Room Temperature (psi)	
	Epon 901/B-1	5180	1 to 2
	X-Epon 99-105-1	1565	5 to 14

B.	<u>Adhesive</u>	Average Tensile	Elongation
		Strength at -320°F (psi)	
	Epon 901/B-1**	8350	1 to 1.5
	X-Epon 99-105-1	11,160	1 to 5.5

* Tensile strength and % elongation in accordance with ASTM-D-638. Epon 901/B-1 cured 1.5 hr at 200°F. X-Epon 99-105-1 specimens cured 30 min. at 140°F, plus ½ hr. at 300°F.

**The Epon 901/B-1 specimens broke in liquid nitrogen under tension within the jaws of the roller-cam jig; final testing was satisfactorily accomplished using a wedge-type jaw.

TABLE X

FLOW CHARACTERISTICS OF X-EPON 99-105-1 EPOXY ADHESIVE

A.	Adhesive <u>Thickness (in.)</u>	Angle of <u>Specimen</u>	Distance of <u>Flow (in.)*</u>
	0.125	60°	0.25
	0.250	60°	1.38
	0.375	60°	2.25

B.	Adhesive <u>Thickness (in.)</u>	Angle of <u>Specimen</u>	Distance of <u>Flow (in.)*</u>
	0.125	90°	0.18
	0.250	90°	2.25
	0.375	90°	3.25

* The flow characteristics of the epoxy adhesive during cure (30 min at 140°F plus ½ hr at 300°F) was determined by measuring the distance of material flow occurring on steel panels held at 60 degree angles and while vertical (90 degree angle).

TABLE XI
COEFFICIENT OF THERMAL EXPANSION
FROM -320°F TO ROOM TEMPERATURE
FOR MACHINED EPOXY SPECIMENS

A.

Adhesive: Epon 901/B-3*

<u>Test Temp.</u> <u>(°F)</u>	<u>Spec. No. 1</u> <u>(in./in. x 10⁻⁶)</u>	<u>Spec. No. 2</u> <u>(in./in. x 10⁻⁶)</u>	<u>Spec. No. 3</u> <u>(in./in. x 10⁻⁶)</u>
-320	---	11.30	9.76
-300	15.64	12.24	10.69
-250	16.80	15.14	12.98
-200	17.82	16.71	15.53
-150	19.09	17.61	17.74
-100	20.32	18.89	19.45
- 50	21.33	19.99	21.30
R.T.	23.37	21.87	22.87

B.

Adhesive: X-Epon 99-150-3**

<u>Test Temp</u> <u>(°F)</u>	<u>Spec. No. 1</u> <u>(in./in. x 10⁻⁶)</u>	<u>Spec. No. 2</u> <u>(in./in. x 10⁻⁶)</u>	<u>Spec. No. 3</u> <u>(in./in. x 10⁻⁶)</u>
-320	25.58	32.51	28.71
-300	26.91	33.45	29.43
-250	31.55	36.13	31.61
-200	36.58	39.25	34.03
-150	42.04	42.97	37.30
-100	50.95	47.69	41.14
- 50	60.40	54.80	46.84
R.T.	75.74	68.91	57.15

* Adhesive cured for 30 min. at 240°F, plus 1.5 hr. at 350°F.

** Adhesive cured for 30 min. at 140°F. plus 1/2 hr at 300°F.

TABLE XII
COEFFICIENT OF THERMAL EXPANSION
FROM -320°F TO ROOM TEMPERATURE
FOR MOLDED EPOXY SPECIMENS

A. <u>Adhesive: Epon 901/B-1*</u>			
<u>Test Temp.</u> <u>(°F)</u>	<u>Spec. No. 1</u> <u>(in./in. x 10⁻⁶)</u>	<u>Spec. No. 2</u> <u>(in./in. x 10⁻⁶)</u>	<u>Spec. No. 3</u> <u>(in./in. x 10⁻⁶)</u>
-320	18.43	18.12	18.32
-300	18.87	18.68	18.78
-250	19.90	19.52	19.75
-200	21.12	20.66	20.93
-150	21.96	21.86	21.95
-100	23.30	22.87	23.25
- 50	24.89	24.29	25.19
R.T.	27.25	25.55	26.99
B. <u>Adhesive: X-Epon 99-105-1**</u>			
<u>Test Temp</u> <u>(°F)</u>	<u>Spec. No. 1</u> <u>(in./in. x 10⁻⁶)</u>	<u>Spec. No. 2</u> <u>(in./in. x 10⁻⁶)</u>	<u>Spec. No. 3</u> <u>(in./in. x 10⁻⁶)</u>
-320	24.19	22.31	22.86
-300	25.08	22.96	23.68
-250	26.26	24.63	25.44
-200	27.88	26.15	27.10
-150	29.55	28.12	29.29
-100	34.56	33.20	34.83
- 50	34.87	33.58	36.09
R.T.	40.57	39.11	43.37

* Adhesive cured 1.5 hr at 200°F.

** Adhesive cured 30 min. at 140°F, plus ½ hr. at 300°F.

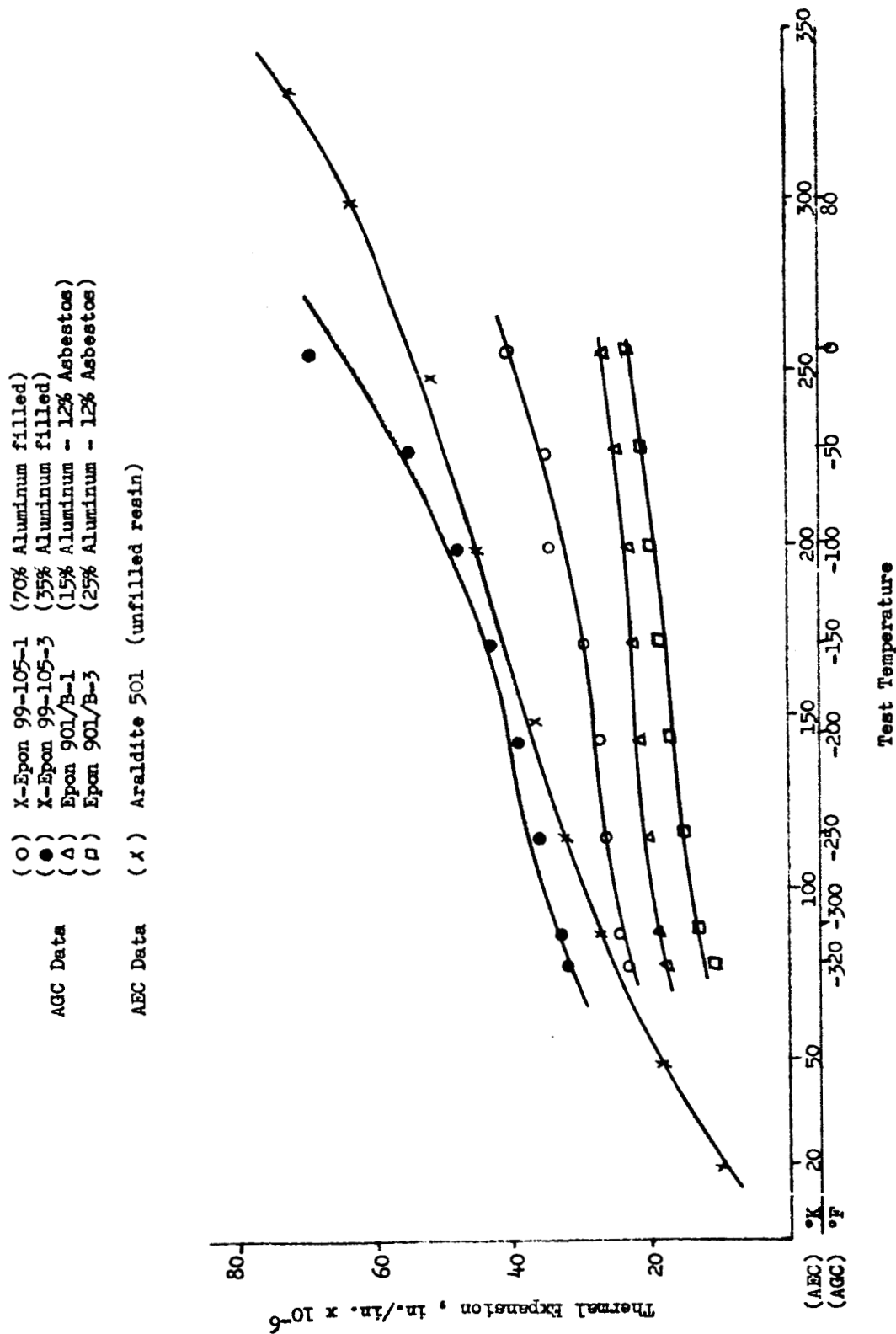


Figure 3

Linear Thermal Expansion Coefficients of Epoxy Materials

4. Tensile elongation data shows the increased flexibility of the Epon 99-105-1 over the Epon 901/B-1 system at both ambient and cryogenic temperatures.

VII. WELDING OF AISI 347 STAINLESS STEEL TO INCONEL 718

The purpose of this investigation was to ascertain the quality of AISI 347 stainless steel to Inconel 718 welds.

Half-inch thick plates of the two materials were TIG welded to each other using Incoweld A, Hastalloy W, and 19-9 WM₀ filler wires. After welding, the plates were processed to provide the following conditions for testing and inspection.

- A. As received, welded and aged.
- B. As received, aged and welded.
- C. As received, welded, solution-annealed, and aged.
- D. As received, welded.

Radiographic and dye penetrant inspection as well as metallographic examination of the welds revealed no defects.

The tensile properties of the weldments were determined and these are listed in Table XIII. The comparative properties of the Inconel 718 and AISI 347 stainless steel parent metals are shown in Table XIV.

In all cases, fracture occurred in the 347 stainless steel parent metal or the weld heat-affected zone at an ultimate stress, which is typical of the 347 stainless steel.

VIII. EVALUATION OF HEAT-REFLECTIVE COATINGS FOR THRUST CHAMBER SUPPORTS

The purpose of this investigation was to select a heat-reflective coating for the thrust chamber supports. Two coatings were evaluated: DA-9 protective coating manufactured by the Markal Company, and Vel-Von 60-3 aluminum paint (formerly known as "Alumicone" 2003) manufactured by Atech, Inc.

The following test conditions were prescribed:

Thermal shock from room temperature into liquid nitrogen (-320°F) temperature,

Flame impingement on coating (approximately 2000°F);

Thermal stability at temperatures of 800°F and 1200°F.

TABLE XIII

**ROOM TEMPERATURE TENSILE PROPERTIES OF
INCONEL 718-347 STAINLESS STEEL WELDMENTS**

Condition	Filler Rod	Ultimate Strength (ksi)	Elongation % in 1-in.	Fracture Location
As received	Incoweld A	96.4	26	347 HAZ
Welded and aged		97.3	23	"
		96.4	25	"
		95.2	29	"
		96.3	25.7	
As received	"	94.9	33	347 PM
Aged and welded		95.2	32	"
		94.1	33.5	"
		93.9	34	"
		94.5	33.1	
As received	"	92.7	33	347 HAZ
Welded		92.9	33	"
Solution annealed		93.4	34	"
aged		92.4	33.5	"
		92.9	33.6	
As received	"	94.9	33	347 PM
Welded		95.2	35	"
		94.7	33	"
		94.9	33.7	

PM = Parent metal
HAZ = Heat affected zone

TABLE XIII (cont'd)

MECHANICAL PROPERTIES OF
INCONEL 718-347 STAINLESS STEEL WELDMENT

<u>Condition</u>	<u>Filler</u>	<u>Ultimate Tensile Strength (ksi)</u>	<u>Elongation % in 1-in.</u>	<u>Fracture Location</u>
As received	Hastalloy W	95.5	30	347 PM
Welded and aged	"	95.2	34	"
		96.2	32	"
		96.6	32	
		95.9	30.8	
As received		94.9	33	347 PM
Aged and welded		93.7	-	Weld
		95.0	35	347 PM
		94.8	34	"
		94.6	34	
As received		94.1	-	Weld
Welded		93.8	30	347 HAZ
Solution annealed and aged "		93.7	32	"
		93.0	-	Weld
		93.7	31	
As received		94.8	36	347 HAZ
Welded		95.0	36	"
		89.9	-	Weld
		94.7	36	347 HAZ
		93.6	36	

PM = Parent metal
HAZ = Heat affected zone

TABLE XIII (cont'd)

MECHANICAL PROPERTIES OF
INCONEL 718-347 STAINLESS STEEL WELDMENT

Condition	Filler	Ultimate		Elongation % in 1-in.	Fracture Location
		Tensile Strength Ksi			
As received Welded and aged	19-9 W Mo	96.4		30	347 PM
		95.9		29	347 PM
		<u>95.5</u>		<u>30</u>	347 PM
		95.9		29.7	
As received	"	93.7		40	347 PM
		93.3		40	347 PM
		93.9		39.5	347 PM
		<u>94.3</u>		<u>41.0</u>	
		93.8		40.1	
As received Welded Solution annealed Aged	"	93.2		35.5	347 PM
		93.8		35	"
		93.2		35	"
		<u>92.5</u>		<u>-</u>	"
		93.2		35.2	
As received Welded	"	96.3		39	347 PM
		95.1		-	
		<u>97.6</u>		<u>36.5</u>	347 PM
		96.3		37.8	

PM = Parent metal

TABLE XIV
TYPICAL PROPERTIES OF 347 STAINLESS STEEL
AND INCONEL 718 ALLOYS

	<u>Tensile Strength</u> <u>Ksi</u>	<u>Yield Strength</u> <u>.2% Offset</u> <u>Ksi</u>	<u>Elongation</u> <u>% in 2-in.</u>
347 Stainless Steel	85	40	60
Inconel 718 Solution annealed	115	60	50
Solution treated and aged	200	165	23

A. LABORATORY INVESTIGATION

1. Ten high carbon tool steel coupons (1-in. by 4-in. by 1/16-in.), were surface abraded and cleaned with trichlorethylene prior to applying the coatings.

Five of the ten coupons were coated with Markal's DA-9 coating (modified epoxy, aluminum filled). Two coats were applied by spray with a 30 min air-dry at room temperature and a 30 min oven cure at 300°F after each coat. The remaining five steel coupons were coated with Atech's Vel-Von-3 coating (silicone, aluminum filled). Two coats were applied by spray with a 30 min air-dry at room temperature and a 30 min oven cure at 400°F after each coat.

2. The Vel-Von specimens were identified by numbers 1 through 5 and the DA-9 specimens were marked with numbers 6 through 10. The results of the exposed specimens are shown in Figure No. 4 and the test conditions described below are summarized in Table XV.

a. Thermal Shock

Room-temperature-conditioned Specimens No. 1 and 6 were subjected to the cryogenic temperature of -320°F by immersion in liquid nitrogen for six minutes. Temperature stabilization of both specimens occurred within one minute.

b. Flame Impingement

Specimens No. 2 and 7 were exposed to the flame (approximately 2000°F) of a Fisher burner (butane gas/air mixture) for a total duration of one minute each. Flame temperatures were checked with a thermocouple and material examinations were made after the end of each 15 sec exposure cycle.

Specimens No. 5 and 10 were exposed to the flame impingement for 15 sec, followed by their immediate immersion into cold tap water. A second 15 sec cycle at the 2000°F flame temperature was made on the same exposed wet specimens.

c. Flash Heat Stability

Specimens No. 3 and 8 were exposed for six minutes at an oven-air temperature of 800°F prior to coating examination.

Specimens No. 4 and 9 were exposed for six minutes at an oven-air temperature of 1200°F prior to coating examination.

3. Review of previous testing data and product literature for the two coating systems indicated:

TABLE XV

THERMAL STABILITY OF HEAT REFLECTIVE COATINGS FROM
TEMPERATURE OF -320°F TO +2000°F

<u>Coating Type</u>	<u>Specimen No.</u>	<u>Exposure Condition</u>	<u>Test Results</u>
<u>Vel-Von 60-3</u> (Alumicon 2003) Silicone-aluminum	1	Liquid nitrogen immersion, 6 min in fluid (1 min to -320°F)	Material cracked and flaked off 5% of sur- face; poor adhesion to steel.
	2	Butane gas-air mixture, flame temperature 2000°F, four 15-sec cycles	15 sec: no apparent effect on material. 30 sec: slight blistering and softening locally 45 sec: No further change 60 sec: Surface blis- tering locally.
	3	Oven heat exposure, 6 min at 800°F	Moderate blistering; material flaked off edges and 10% of one surface; poor adhesion.
	4	Oven heat exposure, 6 min at 1200°F.	Heavy blistering over 75% of surface area; material unchanged where adhered to steel.
	5	15 sec at 2000°F flame temperature into running tap water (70°F)	No apparent effect of flame or thermal shock on coating.
<u>DA-9</u> Epoxy-aluminum	6	Liquid nitrogen immersion, 6 min in fluid (1 min to -320°F).	No effect of exposure.
	7	Butane gas-air mixture, flame temperature 2000°F four 15-sec cycles	15 sec: surface softening and rehardening on cooling 30 sec: smoking; softening of entire coating. 45 sec: coating soft; easily scratched. 60 sec: blistering on edges; discoloration.
	8	Oven heat exposure, 6 min at 800°F	Slight blistering; material discoloration and 5% flake off; poor adhesion in local area.

TABLE XV (Cont'd)

<u>Coating Type</u>	<u>Specimen No.</u>	<u>Exposure Condition</u>	<u>Test Results</u>
<u>DA-9</u> Epoxy-aluminum	9	Oven heat exposure, 6 min at 1200°F	Moderate blistering, material flaked off 10% of surface area; material degradation indicated by tape test.
	10	15 sec at 2000°F flame temperature into running tap water (70°F)	No apparent effect of flame or thermal shock on coating.

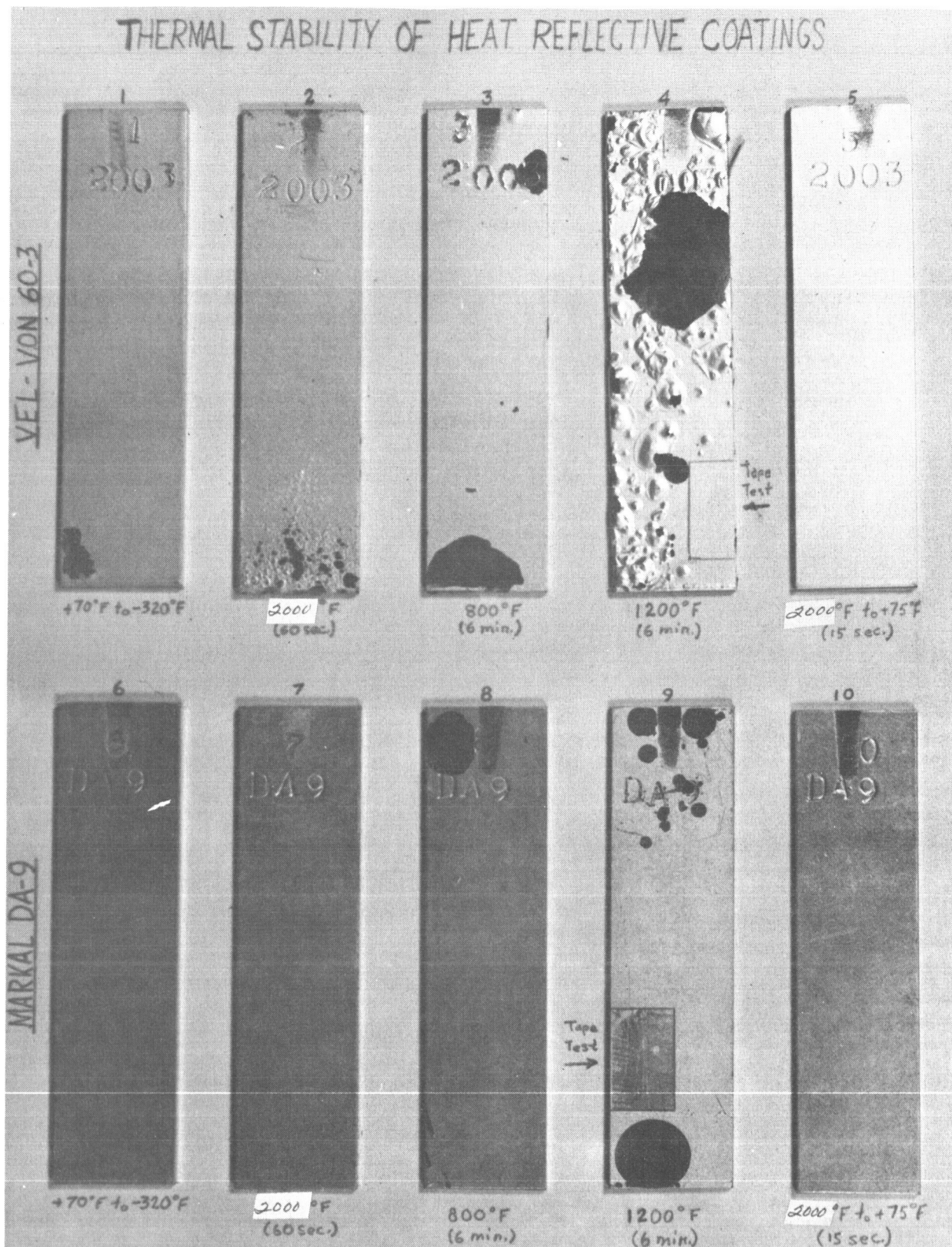


Figure 4

Thermal Stability of Heat-Reflective Coatings

a. DA-9 epoxy coating is satisfactory for limited exposure at 1000°F; the material softened but rehardened to a durable surface after three 70 sec temperature cycles.

b. DA-9 epoxy coating is resistant to a 20% salt spray for 15 hr from room temperature to 100°F.

c. Vel-Von 60-3 coating, after exposure to 1200°F, was reported to be satisfactory for continuous 20% salt spray for 24 hr.

B. PRODUCT LITERATURE SURVEY

The DA-9 coating is reported in Markal Company product literature to be satisfactory for continuous protection against corrosion and atmosphere at 600°F, with intermittent exposures to 720°F.

The results of an independent laboratory report on Atech's Vel-Von 60-3 coating indicates the material surpasses the 900°F temperature and 24 hr salt spray test specified by MIL-P-20087. The test results indicate the Vel-Von 60-3 is satisfactory for continuous 20% salt spray for 24 hr after exposure to 1200°F.

Optimum heat-resistant properties for the Vel-Von coating are obtained by conditioning the specimens at 500°F for two hours after curing, then raising the temperature to 750°F for two more hours, according to Atech's product bulletin. If two coats are desirable, the first coat must be thoroughly cured by subjecting the coating to temperatures up to 1200°F to fuse the aluminum particles to the metal.

C. CONCLUSIONS

Markal's DA-9 coating was unaffected by thermal shock from room temperature into liquid nitrogen (-320°F) and return to ambient; whereas, Atech's Vel Von 60-3 coating showed evidence of flaking when the specimens were returned to ambient temperature.

Results of direct flame impingement indicated both materials are unaffected during a 15 sec exposure to 2000°F or by subsequent water quenching of the "hot" specimens; however, after continual flame impingement, the Vel-Von coating blistered locally and the DA-9 coating softened with resultant hardening upon cooling.

Exposure to flash heat conditions of 800°F and 1200°F indicated the DA-9 epoxy coating had better resistance to blistering than the Vel-Von silicone coating. These results are largely based upon the superior adhesion characteristics of the epoxy over the silicone material. Degradation of the epoxy material at 1200°F was evidenced by a tape peel test; whereas, the silicone material was unaffected.

D. RECOMMENDATIONS

Markal's DA-9 coating is recommended for use as a heat-reflective coating for limited service at high temperatures, not to be exceeded by:

1. Four minutes at 800°F⁽⁵⁾
2. Three minutes at 1000°F
3. One minute at 1200°F⁽⁵⁾
4. Fifteen seconds at 2000°F

The DA-9 coating is marginal for protection against salt spray at temperatures exceeding 100°F; therefore; the use of the DA-9 rust inhibiting primer should be considered for added protection against corrosion.

Further investigation of the specified primer for DA-9, and silicone primer for the Vel-Von coating system is needed for improving the adhesion qualities of both materials.

IX. TORSIONAL PROPERTIES OF INCONEL X-750

This work was conducted to provide design data for the turbopump shaft. Twelve torsional specimens and 18 tensile specimens were machined from Inconel X-750 forgings, heat-treated, and tested at room temperatures and at -320°F. Six torsional and nine tensile samples were tested at each temperature. Both torsion and tension samples were heat-treated prior to final machining. The heat-treating cycle was 1300°F ± 25°F for 20 hr, then cool in still air.

Torsional tests were performed in the Metals Laboratory, Department of Civil Engineering, University of California. A Reihle Torsion Testing Machine was used. Torque versus angle of twist curves for each torsional test were obtained. From these data, the ultimate strength and proportional limit in torsion were calculated (see Table XVI). The torsional ultimate strength was calculated according to the method of Nadai to permit correction for the nonlinear stresses after yield point is passed.

$$\text{Ultimate Shear Stress} = \frac{12X \text{ max. torsional moment}}{\pi D^3}$$

where D is the specimen diameter.

The proportional limit was calculated from the equation:

$$\text{Proportional Limit} = \frac{16X \text{ torsional moment}}{\pi D^3}$$

(5) These limits are conservative values; additional tests would have to be conducted to determine the exact time at temperatures this coating would withstand.

TABLE XVI

TORSIONAL PROPERTIES OF INCONEL X-750 ALLOY
(AGED - 1300°F/20 HR)

<u>Specimen No.</u>	<u>Test Temp °F</u>	<u>Ult. Shear Strength, ksi</u>	<u>Proportional Limit, ksi</u>	<u>Shear Modulus psi</u>	<u>Hardness R_c</u>
4	R.T.	112.3	66.9	9,160,000	31
6	R.T.	115.5	67.3	8,690,000	33
9	R.T.	112.3	70.3	7,670,000	32.5
10	R.T.	113.6	74.2	7,380,000	35
12	R.T.	113.5	72.0	7,950,000	35
	Avg.	113.4	70.14	8,170,000	33.3
1	Approx. -320°F	120.3	78.40	8,720,000	34.0
3	Approx. -320°F	125.0	78.40	9,310,000	32.0
5	Approx. -320°F	122.7	73.30	9,550,000	33.5
7	Approx. -320°F	119.8	67.30	8,810,000	33.0
8	Approx. -320°F	124.6	76.70	8,210,000	33.0
11	Approx. -320°F	124.5	74.90	8,420,000	34.0
	Avg.	123.3	74.83	8,837,000	33.3

The modulus of rigidity, G, from

$$G = \frac{TL}{\phi J}$$

Where T is the torsional moment, L the length, ϕ the angle of twist in length L, and J the polar moment of Inertia.

The -320°F temperature was obtained by wrapping the specimen in insulated paper, soaking in liquid nitrogen, and then inserting the specimen into the testing grips. Liquid nitrogen dripped onto the sample throughout the testing duration.

Tensile test results are shown in Table XVII.

Examination of the results presented in Tables XVI and XVII shows that the average low temperature torsional ultimate strength and proportional limit values increased 8.7% and 6.7% over their respective room temperature averages. At -320°F, the average ultimate tensile strength, 0.2% offset yield strength and percent elongation showed increases of 21.6%, 8.7%, and 10.7%, respectively over their room temperature values. The reduction of area decreased 7.5% at -320°F.

X. DIMENSIONAL STABILITY OF AISI 440C-STAINLESS STEEL

The purpose of this investigation was to establish the dimensional stability of turbopump bearings when subjected to liquid hydrogen temperatures.

The 440C Stainless Steel rollers were removed from the roller bearing assemblies and were dimensionally measured and tested for retained austenite content. These bearings were heat-treated to a hardness of 58 Rockwell C minimum and were subjected to a sub-zero treatment between quenching and tempering to minimize the retained austenite content.

A. INVESTIGATION RESULTS

Results of dimensional measurements and retained austenite determinations are shown in Tables XVIII and XIX, respectively. The following schedule was used for this investigation:

1. Measure three bearing rollers, two places each.
2. Determine by nondestructive test the percentage of retained austenite in each roller.
3. Soak rollers for two hours at -100°F.
4. Measure the three rollers at the same two places on each roller.
5. Same as Step 2 above.

TABLE XVII

TENSILE PROPERTIES OF INCONEL X-750 ALLOY
(AGED - 1300°F/20 HOURS)

Specimen No.	Test Temp °F	Ult. Tensile Strength ksi	.2% Offset Yield Strength ksi	Elongation in 4D %	Red. of Area %
1	R.T.	171.0	121.5	25	37.7
3	R.T.	170.5	121.5	24	34.6
5	R.T.	171.0	123.0	24	35.2
7	R.T.	175.5	122.0	24	30.8
9	R.T.	171.0	119.5	25	32.1
11	R.T.	164.5	116.5	24	32.1
14	R.T.	175.0	121.5	27	40.8
16	R.T.	171.5	118.0	25	35.3
17	R.T.	170.5	117.5	29	34.6
	Avg.	171.0	120.0	25.2	34.8
2	-320	200.0	130.5	28.2	37.7
4	-320	204.5	131.5	27.1	32.1
6	-320	211.5	130.0	28.7	30.6
8	-320	211.5	129.5	29.7	34.6
10	-320	205.5	131.5	26.0	30.6
12	-320	210.0	130.5	30.4	30.0
13	-320	214.0	134.0	24.1	29.3
15	-320	212.5	132.0	31.8	37.2
18	-320	202.0	126.5	25.1	28.1
	Avg.	207.9	130.7	27.9	32.2

TABLE XVIII

DIMENSIONS OF AISI 440C STAINLESS STEEL ROLLER BEARINGS
AFTER SOAKING AT VARIOUS CRYOGENIC TEMPERATURES

	Diameter			Length		
	Bearing: #1	#2	#3	#1	#2	#3
Removed from Pump Assembly	.578189	.578184	.578186	.698790	.698785	.698775
After 2 Hr @ -100°F	.578185	.578180	.578180	*	*	*
After 2 Hr @ -320°F	•	*	•	*	•	•
After 2 Hr @ -423°F	.578185	.578180	.578180	.699974	.699975	.699972
Net Change in Dimension between removal from TPA and after -423°F soaking.	-.000005	-.000004	-.000006	+.001184	+.001190	+.001197

•Measurements not supplied

TABLE XIX

RETAINED AUSTENITE VS. LOW TEMPERATURE
EXPOSURE FOR HEAT-TREATED AISI 440C STAINLESS STEEL ROLLER BEARINGS

Roller Bearing	<u>Retained Austenite, %</u>		
	<u>#1</u>	<u>#2</u>	<u>#3</u>
As Removed from TPA	4	3.6	3.5
After 2 Hr @ -100°F	4	3.0	4.5
After 2 Hr @ -320°F	3.5	2.8	2.8
After 2 Hr @ -423°F	3.5	2.6	1.2
Net Change between removal from TPA and after -423°F soaking.	-0.5	-1.0	-2.3

6. Soak rollers for two hours at -320°F .
7. Same as Step 4 above.
8. Same as Step 2 above.
9. Soak rollers for two hours at -423°F .
10. Same as Step 4 above.
11. Same as Step 2 above.

Retained austenite content was determined by X-ray diffraction. The results presented in Table XVIII show an increase in length of 0.001184-in. to 0.001197-in. in the rollers after soaking at cryogenic temperatures. There was a negligible change in the diameters of these rollers. The above phenomenon can be attributed to the transformation of the retained austenite in the heat-treated 440C stainless steel to martensitic structure and to the orientation of the retained austenite in the rolling direction of the bar from which the rollers were machined.

The data presented in Table XIX shows a correlation between decreasing austenite content and the growth of the rollers listed in Table XVIII.

B. CONCLUSIONS

The retained austenite content and the orientation of the grain in the rolling direction were found to have a definite effect upon the dimensional stability of the heat-treated 440C stainless steel roller bearings. Stability can be improved by subjecting the bearings to extreme cryogenic temperatures. Information in literature indicates that the low temperature treatment should be applied as soon as possible after quenching.

C. RECOMMENDATION

Heat-treated 440C Stainless Steel used for cryogenic bearing applications should be dimensionally stabilized at extreme low temperatures as soon as possible after quenching and before tempering.

XI. RIGIMESH MECHANICAL PROPERTIES AND FABRICATION CHARACTERISTICS

The purpose of this investigation was to determine the mechanical properties and fabrication characteristics of Rigimesh, a porous metal sheet and plate product manufactured by the Aircraft Porous Media Company. Rigimesh was used for the M-1 injector plate and was under consideration for use in the fabrication of transpiration cooled injector baffles.

A. MECHANICAL AND PHYSICAL PROPERTIES

The room temperature mechanical properties of the 0.125-in. 347 stainless steel porous metal sheet were determined in the woof, warp, and 45 degree directions. Typical fractures for each condition are illustrated in Figure No. 5 and the test results, which are the averages based upon four samples tested in each of three directions are listed in Table XXI. The flow characteristics of the sheet were identified by the supplier as providing a flow of 120 SCFM at a pressure drop of 2 psi.

It is significant that the mechanical properties of the porous sheet are not as dependent upon the direction of test as might be expected. Examination of photomicrographs (Figure No. 6) shows the existence of a metallurgical bond between adjacent intersecting woof and warp wires. This bond develops after sintering the compacted sheet and contributes significantly to the strength of the porous sheet. This is demonstrated by the fact that in the 45-degree cut samples, where neither woof nor warp wires run continuously through a sample, there is only a small dip in the yield strength in relationship to that obtained in the two principal directions.

The individual wires in the sheet are in a "dead soft" condition. Tukon Hardness converted to Rockwell B shows wire hardness to be R_b 70 to R_b 84.

The coefficients of thermal expansion were determined for the temperature range of 70°F to 2000°F. The results are shown in Table XX.

B. DETERMINATION OF PROCESS CHARACTERISTICS

1. Vendor's Manufacturing Processes

Aside from information given by the supplier, little is known about the vendor's manufacturing process. The material is developed upon the basis of a specific ΔP value and all product controls are set to achieve this value. The manufacture of porous metal is by a batch-type process, and the size of sheet is limited to a maximum of 18-in. by 24-in. because of equipment limitations. Cleanliness of the porous sheet is maintained by controlling each manufacturing step and by the final sintering, which is done in a protective atmosphere.

The supplier has indicated that the porous sheet must be protected from contamination during all phases of fabrication. Several samples of porous metal sheet were deliberately contaminated by immersing them in cutting oil prior to cleaning them to a condition that was compatible with liquid oxygen and gaseous oxygen systems. Analysis of the two cleaned 4-in. by 6-in. panels showed a residual hydrocarbon content of 1.3 mg/ft² and 1.7 mg/ft², respectively; these values are well within the allowable contaminating limits of the applicable specification.

TABLE XX.
THERMAL EXPANSION OF RIGIMESH

<u>Temperature Range</u>	<u>347 Stainless Steel Stock</u>	<u>Direction of Test</u>	
		<u>Woof Cut Porous Sheet in./in./°F</u>	<u>Warp Cut Porous Sheet in./in./°F</u>
RT to 100°F	--	7.02×10^{-6}	7.46×10^{-6}
RT to 500°F	9.5×10^{-6}	9.49×10^{-6}	9.70×10^{-6}
RT to 1000°F	--	10.10×10^{-6}	10.09×10^{-6}
RT to 1500°F	--	10.43×10^{-6}	10.42×10^{-6}
RT to 2000°F	11.2×10^{-6}	10.52×10^{-6}	10.59×10^{-6}

TABLE XXI

MECHANICAL PROPERTIES OF 0.125-IN. RIGIMESH SHEET

	<u>Direction of Test</u>			<u>Annealed 347 Sheet Typicals</u>
	<u>Woof</u>	<u>Warp</u>	<u>45°</u>	
Ultimate tensile strength (ksi)	38.3	36.6	36.3	85.0
Yield strength (ksi)	19.0	18.1	14.0	35.0
Percent Elongation (in./3-in.)	11.8	14.9	27.5	45/55

The modulus of elasticity obtained from analysis of the stress-strain curves was determined to be 13.7×10^6 or about half that of comparable sheet material.

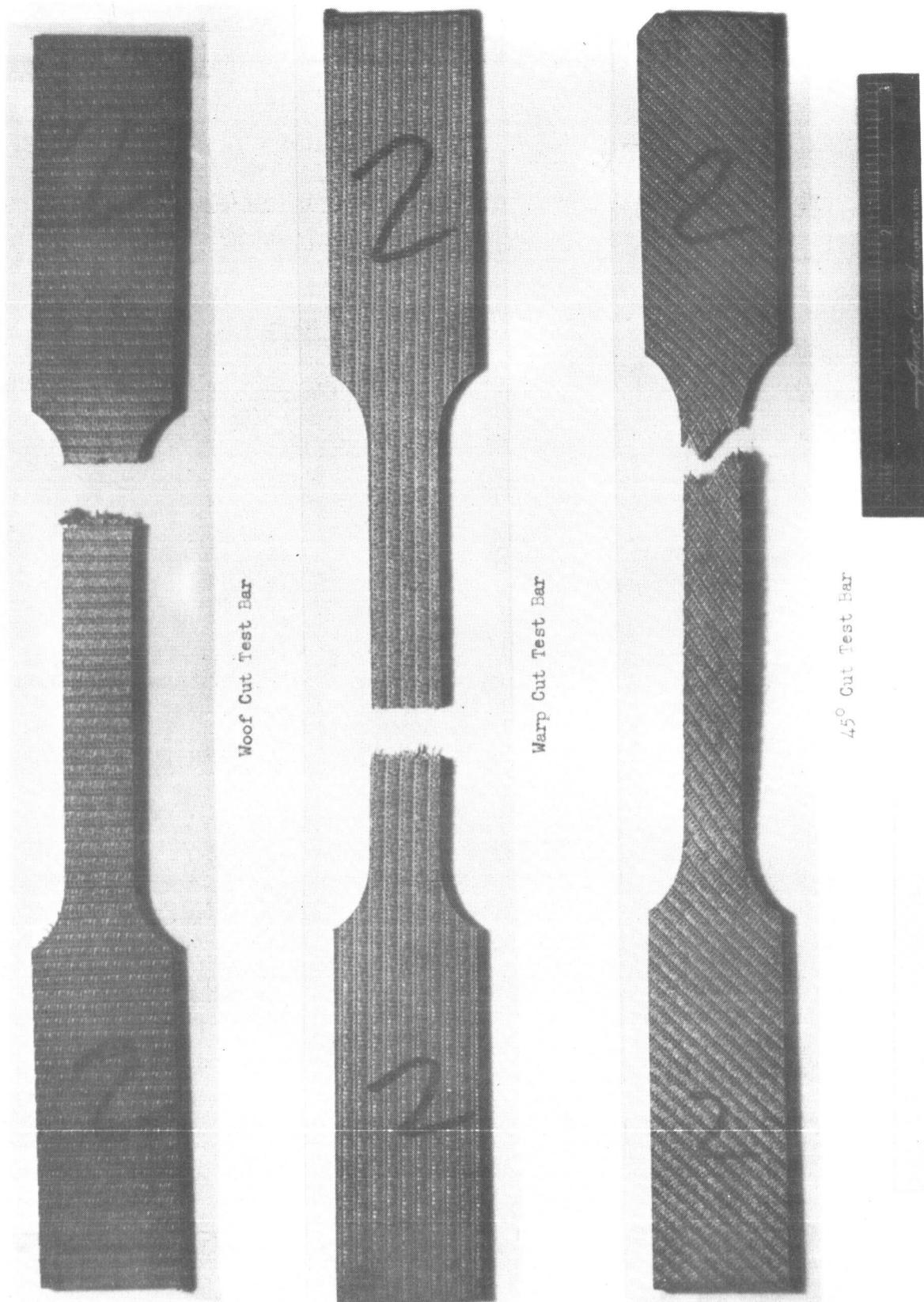
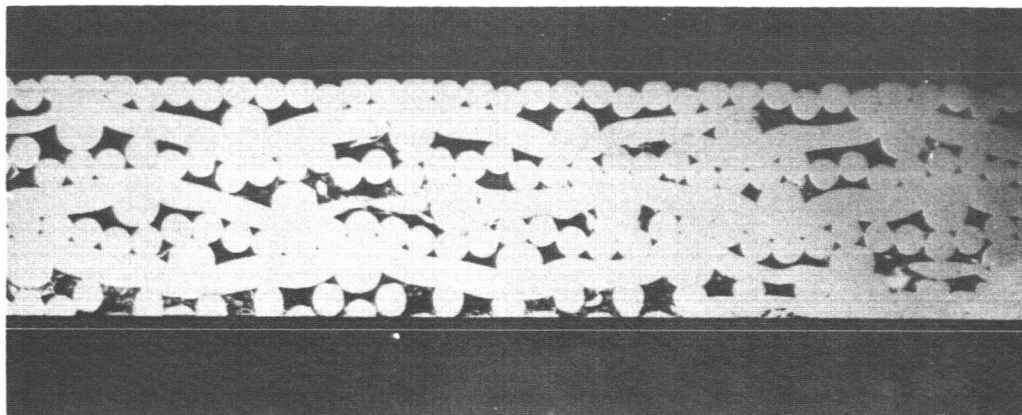


Figure 5

Test Bars Showing Typical Fracture of Rigimesh



Section of Porous Metal Sheet Across Woof (10X)

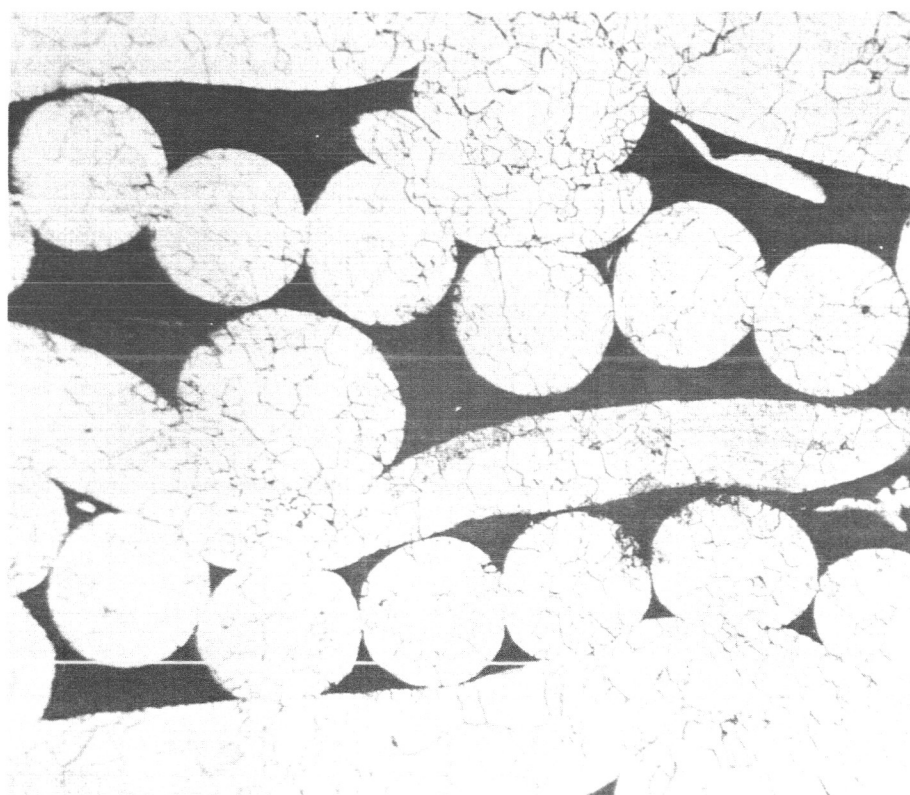


Figure 6. Section of Porous Metal Sheet Across Woof, Polished and Etched. Note Recrystallization and Growth Between Intersecting Woof and Warp Wires. (50X)

2. Welding

Two separate weld studies were conducted. The first study involved the tungsten-inert-gas (TIG) welding of Rigimesh to itself and Rigimesh to 347 stainless steel sheet of equivalent thickness as well as electron-beam (EB) welding of Rigimesh to 347 stainless steel sheet of equivalent thickness. The second study was conducted to establish the feasibility of fabricating Rigimesh injector baffles by the TIG and EB welding processes.

The results of the initial investigation are shown in Table XXII. These results indicate that the ultimate strength of butt-welded, porous-metal joints (porous-to-porous and porous-to-sheet) approximates that of the parent porous sheet; the yield strength increases slightly and the elongation drops to between 50 and 60% of the parent material. Little or no correlation is apparent between thread direction and joint strength. Aside from bead width, the EB-welded sample does not appear to show any advantage over the TIG samples. The welds are illustrated in Figures No. 7, No. 8, and No. 9.

The baffle-welding investigation consisted of fabricating two Rigimesh sandwich baffle specimens using the TIG process to join spacers to one set of Rigimesh panels and using the EB process to weld spacers to the mating set of panels (see Figures No. 10 and No. 11). The spacers were then EB-welded together to form the sandwich baffles. Metallographic examination of the welds revealed cracks in the spacer weld nuggets and at the intersection of several Rigimesh pores and the weld nugget (Figure No. 12). The weld cracks in the spacer nuggets are of a magnitude usually encountered when EB welding AISI 347 stainless steel. AISI 304L stainless steel is less crack-sensitive and should be used for this application. Additional development work is required to eliminate cracking found in the Rigimesh welds.

3. Furnace Brazing

Furnace brazing of porous metal sheet is not recommended because the braze alloy readily diffuses into the porous metal. The use of various "braze-stop-off" materials were investigated with no success (Figure No. 13).

4. Forming and Machining

a. Shearing

The 0.125-in.-thick porous sheet shears cleanly if the sheet is clamped rigidly near the blade.

b. Bending

The results of room temperature bend tests indicate a minimum bend radius of one inch for the particular material tested; however, a much greater bend radius is required when flow characteristics through the bend are to be considered.

TABLE XXII

MECHANICAL PROPERTIES OF TIG- AND EB-WELDED RIGIMESH

<u>Type of Welding</u>	<u>Type of Joint</u>	<u>Test Combination</u>	<u>Ultimate Tensile Strength (ksi)</u>	<u>0.2% Offset Yield Strength (ksi)</u>	<u>Elong. (% in/2-in.)</u>	<u>Reduction in Area, %</u>
T.I.G.	Butt	Warp Cut Porous to 347 S.S. Sheet	37.2	22.7	6.7	9.6
T.I.G.	Butt	Woof Cut Porous to 347 S.S. Sheet	36.5	22.9	5.7	10.7
T.I.G.	Butt	Woof Cut Porous to Woof Cut Porous	34.3	20.6	6.9	12.7
T.I.G.	Butt	Warp Cut Porous to Warp Cut Porous	34.6	20.5	8.4	11.7
Electron Beam	Butt	Woof Cut Porous to 347 S.S. Sheet	38.1	20.6	7.0	8.5
T.I.G.	Butt	347 S.S. Sheet to 347 S.S. Sheet	86.5	52.3	39.0	52.5
T.I.G.	Lap	Warp Cut Porous to 347 S.S. Sheet	33.1	16.7	4.9	3.8
Mechanical Properties of Parent Porous Sheet						
		(Woof)	38.3	19.0	11.8	--
		(Warp)	36.6	18.1	14.9	--

*Values represent weighed Average of 5 Test Samples

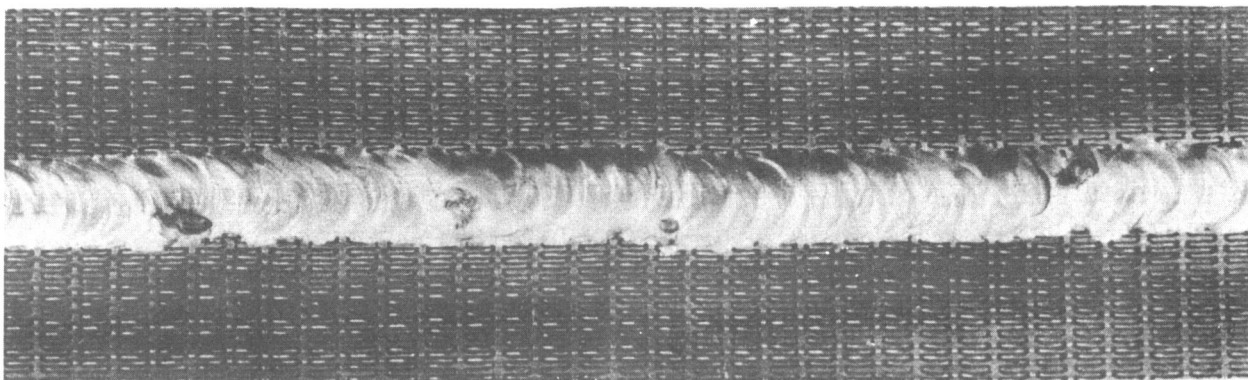


Figure 7. Butt Weld (TIG) Woof to Woof 1.6X. Notice indications of foreign material boil out - 4 Places

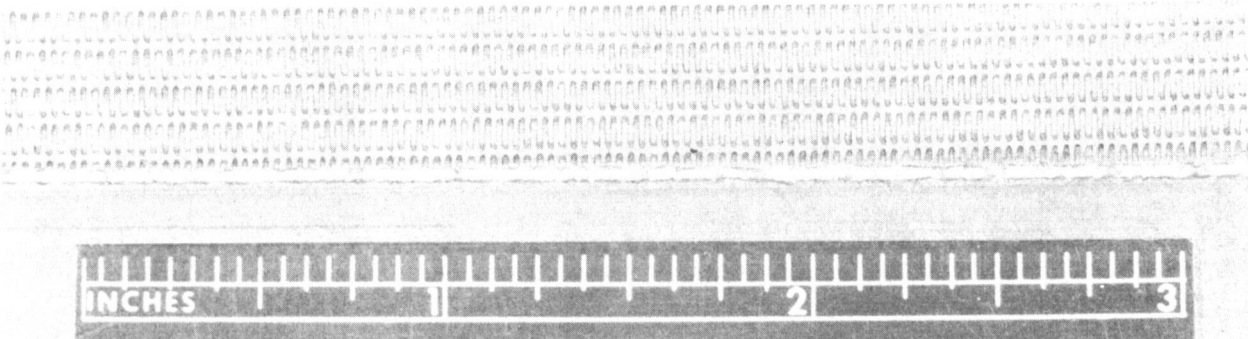


Figure 8. Butt Weld (Electron Beam) Warp to Sheet 1.6X

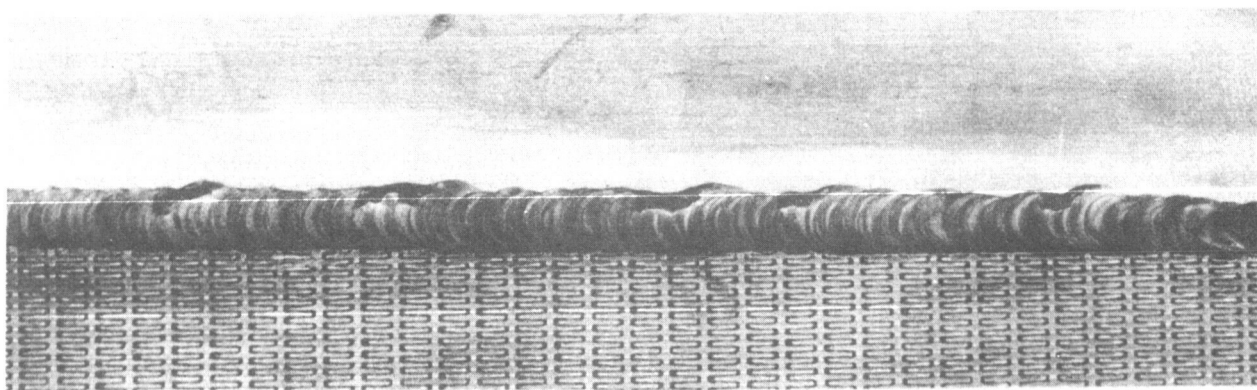


Figure 9. Butt Welded (TIG) Woof to Sheet 1.6X

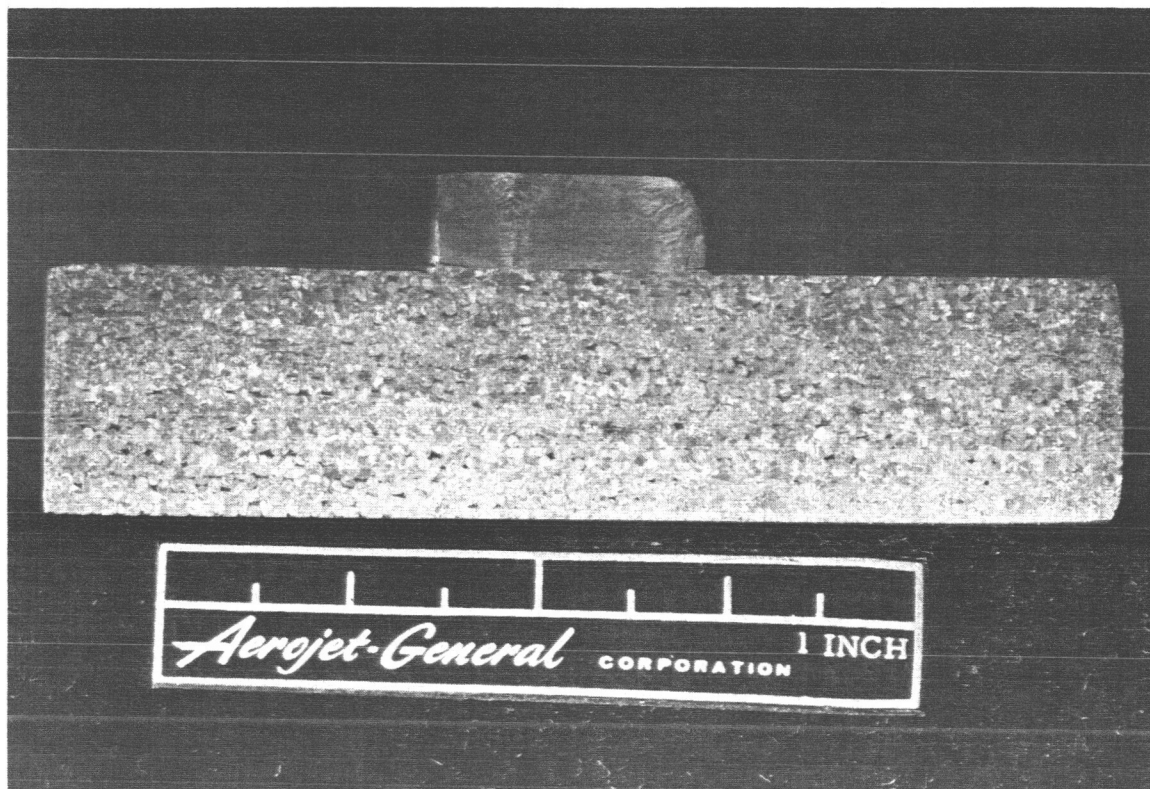


Figure 10

Macrograph of AISI 347 Stainless Steel Spacer Welded to
AISI 347 Stainless Rigimesh Sheet by the Electron-Beam Process

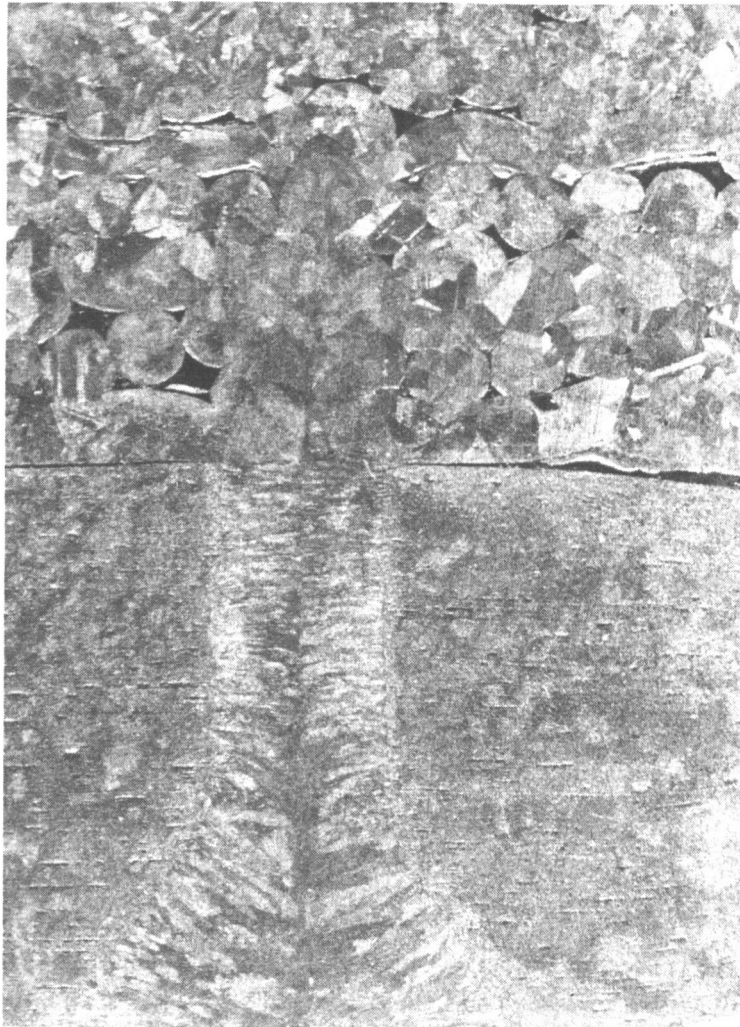


Figure 11

Photomicrograph of AISI 347 Stainless Steel Sheet Welded
to AISI 347 Stainless Steel Rigimesh Sheet by the Electron-Beam Process (24X)

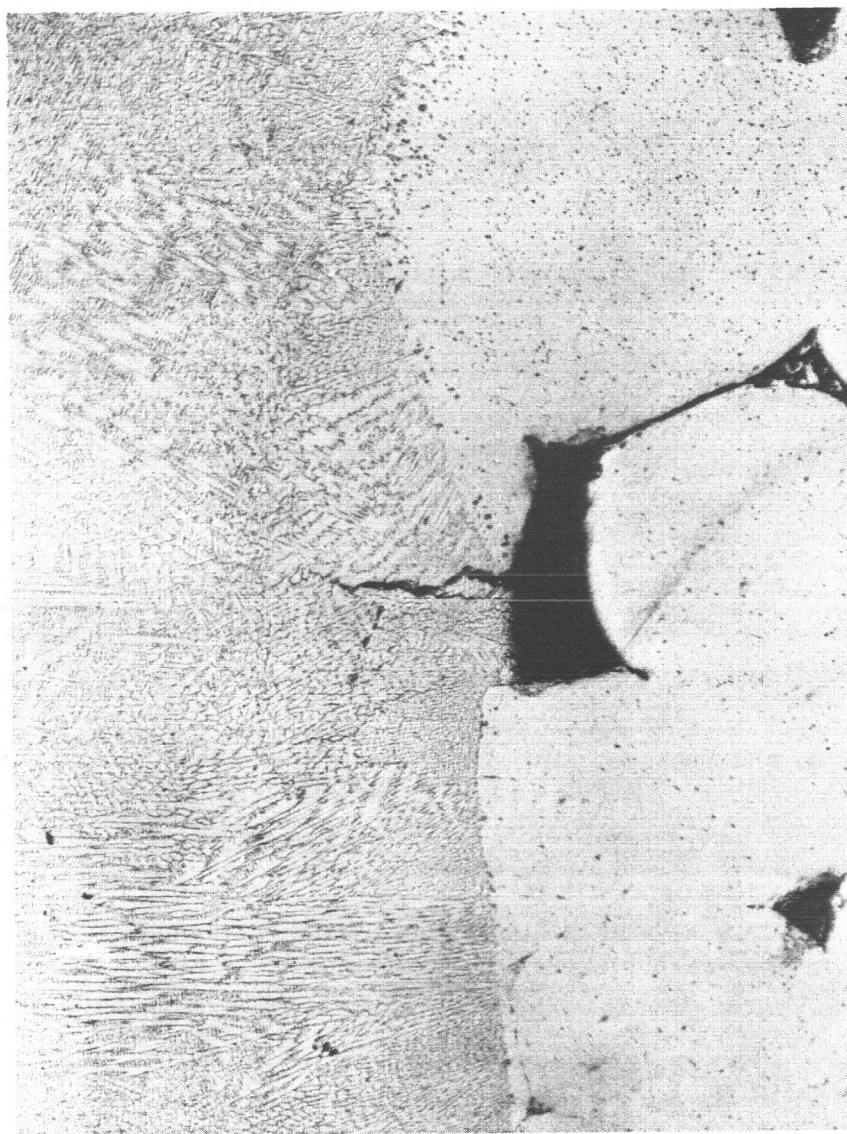


Figure 12

Photomicrograph of Electron-Beam Weld in Rigimesh Showing
Cracking at a Nugget-Pore Intersection (100X)

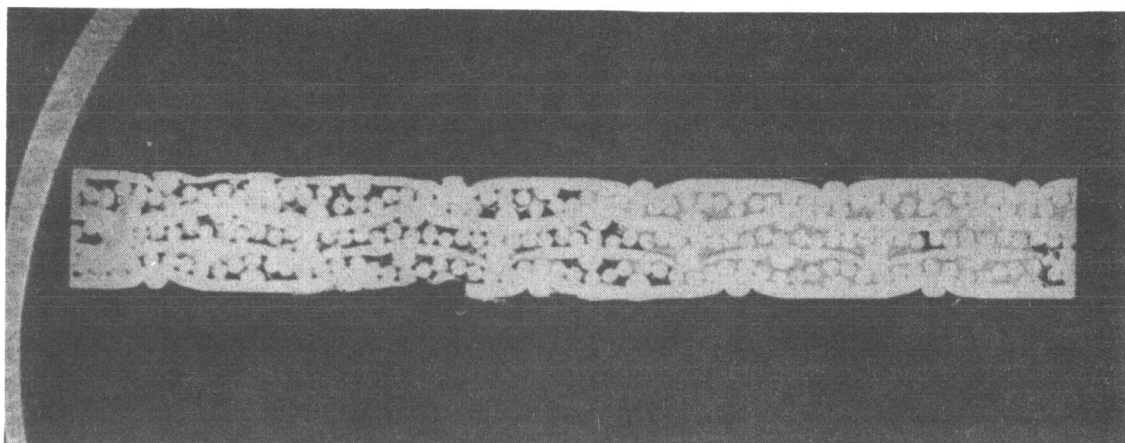


Figure 13

Braze Alloy Penetration into Porous Metal Sheet (5X)

5. Sawing

During the preparation of samples for test, all porous metal sheet cut with a band saw showed delamination along the sawed edge. In addition, one piece of sheet snagged on the blade and delaminated over a six-inch-diameter area. Extreme care should be exercised when sawing this material; and all sawed edges should be subsequently machined.

6. Machining

a. No special problems were encountered when machining the porous metal test pieces. Both cutting and grinding were done without a coolant to minimize contamination.

b. Elox was evaluated against conventional techniques as a method of producing large diameter holes ($3/4$ -in.) in the 0.125-in.-thick porous sheet.

Two sets of holes were drilled in a test plate using both Elox and a conventional end-mill cutter; one hole in each set was perpendicular to the sheet, while the other hole was made at an angle of 45 degrees.

The set-up time for the eloxed holes was 70 minutes per hole with a cutting time of approximately 20 minutes per hole. Set-up time for the end-milled holes was 10 minutes per hole with a drill time of two minutes per hole.

An examination of the two sets of holes after drilling showed the eloxed holes to be cleanly cut with no metal smear around the inside of the hole and little or no burr on the exit side. However, the end-milled holes showed extensive metal smear on the inside hole surface with a pronounced burr on the exit side. In addition to this over-all burr condition, the end-milled 45-degree hole showed a small chip or tear on the back edge. The end-milled holes were cut without coolant, whereas the eloxed samples were immersed in oil.

XII. LARGE TITANIUM 5Al-2.5Sn-ELI PUMP INDUCER FORGING EVALUATION

The purpose of this investigation was first, to establish the low-temperature mechanical properties of the fuel inducer forging of alpha titanium alloy (Ti-5Al-2.5Sn ELI) for design information. Then, to compare the wrought titanium alloy properties with those of the 7079-T652 aluminum fuel inducer and an alpha Ti-5Al-2.5SnELI casting (see section XVII).

The billet supplier was Titanium Metals Corporation of America. The hand forging was produced on an open hammer using conventional techniques. Dimensions of the finished product were 20.0-in. diameter by 13.0-in. high.

A. PROCEDURE

One test section (20.0-in. diameter by approximately 2.5-in.) was parted from the forging.

Smooth and notched tensile specimens (stress concentration K_t of 6.3) of radial and tangential orientations were machined from the test section. Specimens were taken from approximately the mid-radius and mid-thickness locations of the test section.

Tests were conducted at ambient temperature and -423°F . Smooth specimens were measured for ultimate strength, 0.2% offset yield strength, elongation, and reduction of area. Notched specimens were evaluated for ultimate strength. The strain rate was approximately 0.005 in./in./min.

Chemical as well as macro- and micro-analyses were performed.

B. RESULTS

1. Smooth Bar Properties

The data listed in Table XXIII show that strength is increased with decreasing temperature, while ductilities are lowered. The general findings are similar to those reported for the cast 5Al-2.5SnELI grade (see Section XIII). A slight degree of anisotropy is evident from these data. The radial ultimate strength and the 0.2% offset yield strength slightly exceed tangential values, while tangential reduction of area exceeded radial values at room temperature. Elongation values are essentially equivalent. The variance of strength and ductility, at -423°F , was less pronounced than at room temperature.

Table XXIV presents the yield strength-to-density ratios of the Type 5Al-2.5SnELI casting and forging and the Type 7079-T652 aluminum alloy forging as functions of temperature. It is apparent from the data that the wrought titanium alloy is superior at -423°F .

2. Notch Properties

The general behavior of the notched tensile specimens (see Table XXIII) with decreasing temperature is typical (i.e., strength increases at the expense of smooth-bar ductility).

3. Notch Bar-to-Smooth Bar Tensile and Yield Ratios

The ratios shown (Table XXIII) exceed unity at a notch acuity of 6.3. The ratios decrease with decreasing temperature. The wrought alloy has a high degree of notch-toughness at temperatures of ambient and -423°F .

TABLE XXIII

TENSILE PROPERTIES OF ALPHA TITANIUM ALLOY (Ti-5Al-2.5Sn-ELI)
FUEL INDUCER FORGING BLANK

<u>Specimen</u>	<u>Orientation</u>	<u>Test Temp (°F)</u>	<u>Ultimate Strength (ksi)</u>	<u>0.2% Offset Yield Strength (ksi)</u>	<u>Elongation (% in 4D)</u>	<u>Reduction of Area (%)</u>	<u>Notched Tensile Ratio</u>	<u>Notched Yield Ratio</u>
1	Radial	Room	109.4	102.1	11.5	22.0		
2	Radial	Room	111.2	105.6	13.0	17.6		
	Avg.		110.3	103.9	12.3	19.8		
7	Radial	Room	151.3	Notched tensile specimen				
8	Radial	Room	148.5	Notched tensile specimen				
9	Radial	Room	152.9	Notched tensile specimen				
	Avg.		150.9				1.37	1.45
13	Tangential	Room	103.5	97.3	11.0	28.4		
14	Tangential	Room	106.6	98.4	12.5	29.3		
	Avg.		105.1	97.9	11.8	28.9		
19	Tangential	Room	147.8	Notched tensile specimen				
20	Tangential	Room	146.9	Notched tensile specimen				
21	Tangential	Room	157.2	Notched tensile specimen				
	Avg.		150.6				1.43	1.54
4	Radial	-423	198.0	173.8	8.0	14.5		
5	Radial	-423	200.0	175.9	10.0	16.0		
	Avg.		199.0	174.9	9.0	15.8		
10	Radial	-423	235.5	Notched tensile specimen				
11	Radial	-423	239.5	Notched tensile specimen				
12	Radial	-423	231.5	Notched tensile specimen				
	Avg.		235.5				1.18	1.35
17	Tangential	-423	196.0	175.8	6.0	14.1		
18	Tangential	-423	200.5	171.5	10.5	16.8		
	Avg.		198.3	173.7	8.3	15.5		
22	Tangential	-423	224.0	Notched tensile specimen				
23	Tangential	-423	239.8	Notched tensile specimen				
	Avg.		231.9				1.17	1.33

TABLE XXIV

YIELD STRENGTH (0.2% OFFSET)-TO-DENSITY RATIO °F
PUMP INDUCER MATERIALS

<u>Temp (°F)</u>	<u>Cast 5Al-2.5Sn-ELI</u> <u>Titanium Alloy</u>	<u>Wrought 5Al-2.5Sn-ELI</u> <u>Titanium Alloy</u>	<u>Wrought 7079-T652</u> <u>Aluminum Alloy</u>
R.T.	642	625	455
-423	998	1090	596

4. Chemistry

As shown in Table XXV, the carbon and nitrogen levels are slightly more than specification limits. The slight variations in carbon and nitrogen levels are not considered to significantly affect the properties of the forging in this case. However, high interstitial levels should be avoided to attain optimum cryogenic properties.

5. Microstructure

The desired microstructure for optimum toughness, in the alpha titanium alloy, is an equiaxed pattern. As shown in Figure No. 14, this was not achieved in this large forging (20.0-in. diameter by 13.0-in. thick). The structure is not equiaxed; it is dendritic and coarse. This structure is apparently attendant to the forging operation, which either did not sufficiently hot-work the forging or which was carried out at a temperature that was too high. The grain pattern obtained in the large forging did not result in optimum strength and ductility. Improved grain size and forging control should be exercised in future parts to obtain better cryogenic mechanical properties.

C. CONCLUSIONS

The Ti-5Al-2.5SnELI titanium alloy forging exhibited high notched strength and smooth-bar yield strength and ductility at -423°F. Based upon these mechanical property characteristics, the forging is considered very promising for the fuel inducer application.

The forging properties can be improved by controlling forging practice and grain size. The structure was generally coarse, dendritic, and duplex. The preferred structure is uniform, equiaxed grain orientation.

Because of its mechanical properties, the wrought titanium alloy is considered to be a better material than wrought 7079-T652 aluminum and cast titanium 5Al-2.5SnELI alloy.

D. RECOMMENDATION

The fatigue properties of the forging should be established to complete the preliminary evaluation

XIII. CAST TITANIUM 5Al-2.5Sn-ELI PUMP INDUCER EVALUATION

A simulated fuel pump inducer casting of 5Al-2.5Sn-ELI titanium alloy was produced by Oregon Metallurgical Corp., Albany, Oregon.

The experimental work described in this report was performed for three reasons: to establish the vane-section mechanical properties; to study the weld repairability of the alloy using the TIG welding process and to compare the properties of titanium

TABLE XXV

CHEMICAL ANALYSIS OF Ti-5Al-2.5 Sn-ELI FORGING

<u>Element</u>	<u>Forging (Weight %)</u>	<u>Recommended Chemistry (%)</u>
O ₂	0.086	0.12 max
H ₂	0.002	0.0125 max
C	0.063	0.05 max
Fe	0.08	0.25 max
N ₂	0.047	0.04 max
Al	4.9	4.75/5.75
Sn	2.6	2.2/2.8
Mn, V, Mo, Cr	< 0.10 each	0.10 max. each



Magnification: 100X

Etchant: Kroll's

The microstructure is non-equiaxed, coarse, and dendritic. Mechanical properties would be improved if the structure were equiaxed alpha.

Figure 14

Microstructure of Titanium Alloy 5Al-2.5Sn-ELI Pump Inducer Forging

alloy with the properties of the 7079-T652 fuel-inducer forging. The latter alloy is currently used for the fuel pump inducer.

A. PROCEDURE

1. Production of Casting (Oregon Metallurgical Corp.)

Patterns were made to simulate the M-1 fuel inducer. Horizontal vanes were designed in lieu of spiral vanes to minimize tooling costs. Vanes were approximately 0.5-in. thick and over-all diameter was approximately 18-in. (see Figures No. 15 and No. 16).

Molds were prepared by ramming the standard graphite powder, pitch, cement, and water mixture around wooden pattern equipment. The bottom-gated molds were cured and placed in the vacuum-casting furnace. The furnace was evacuated. The simulated inducer was centripetal-cast in the vacuum furnace with the hub-section poured solid. The mold was parted from the inducer casting and the casting was shot-blasted. The casting was annealed (1500°F for two hours) and again shot-blasted.

2. Tensile Specimen Preparation, Radiography, and Testing

Smooth and notched tensile specimens were machined radially and tangentially from Vane F (see Figure No. 16).

Specimens were radiographed. The films obtained were compared with ASTM E 192-62T standards for quality level.

Smooth specimens were tested for ultimate strength, 0.2% offset yield strength, elongation, and reduction of area in accordance with Federal Standard 151. Notched specimens, with stress concentrations of 6.3 to 9.5, were tested for ultimate strength. Tests were conducted at room temperature, -320°F, and -423°F.

3. Metallographic Examination

The vane and fractured specimens were macroexamined and micro-examined for grain pattern, size, and general structure. The titanium-carbon (graphite mold) interaction zone was studied.

4. Chemistry

A chemical analysis was performed for interstitial and alloy contents.

5. Weld Repair Study

Plug welds were introduced into sound base metal and inspected for soundness. This was performed by Oregon Metallurgical Corporation.

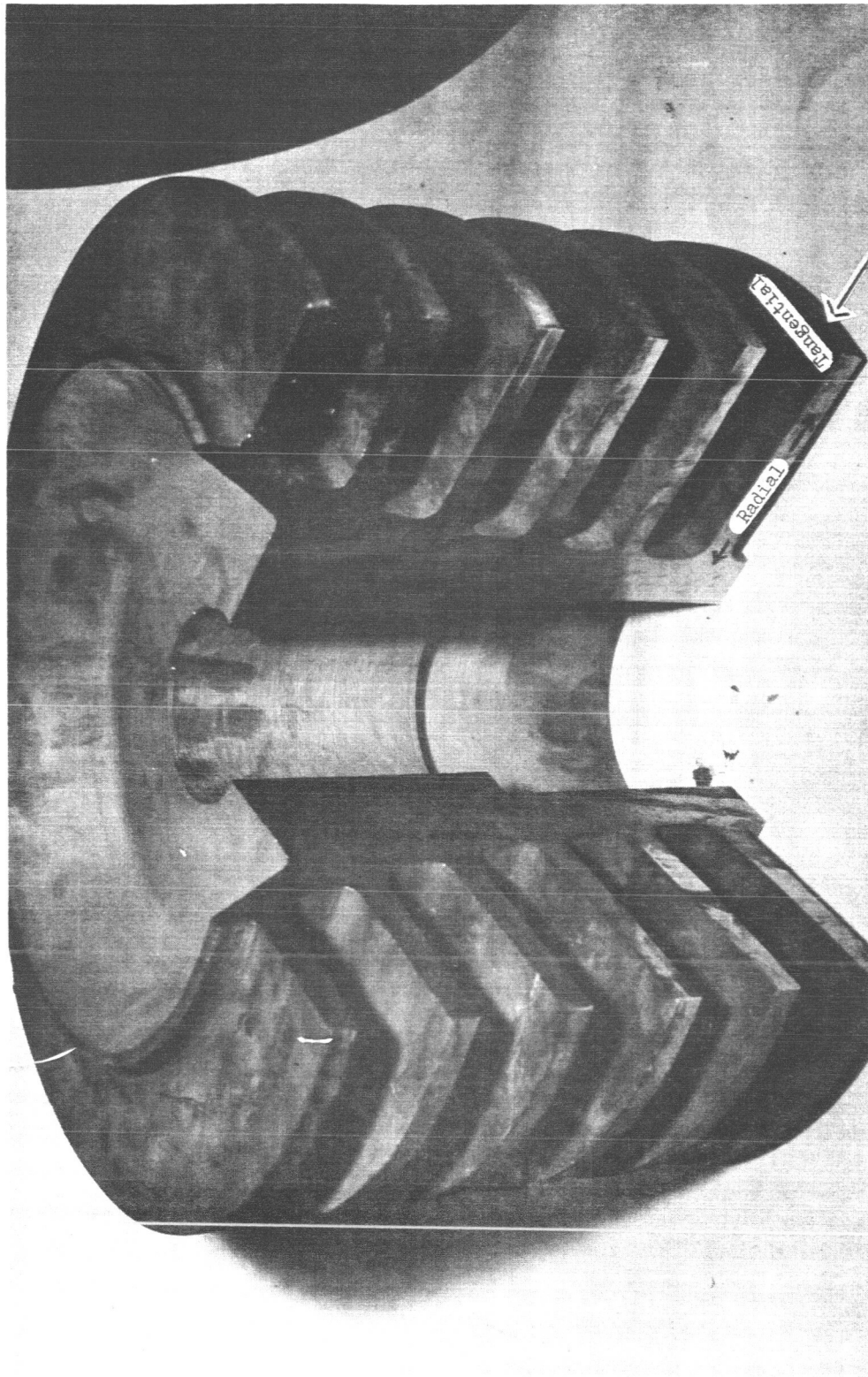


Figure 15

Simulated Fuel Pump Inducer Casting of Titanium Alloy 5Al-2.5Sn-ELI

Drill-hole locations are listed below (see Figure No. 16)

- a. A 1/4-in., drilled through hole was made and repair-welded in Vane A.
- b. A 3/8-in. hole was drilled 1/2-in. deep, and welded at the junction of Vane A and the hub section.
- c. A 3/4-in. hole was drilled 1/2-in. deep, and welded at the junction of Vane B and the hub section.
- d. A 1-1/2-in. access hole was made to accomplish the above weld repair (No. 3).
- e. A 1/2-in. hole was drilled 1/2-in. deep, and welded in Vane F.

Drilled holes were plug-welded in an inert atmosphere using the TIG welding process. Weld rod was rolled from a cast bar from the same heat used in producing the casting. Chill blocks were not used. Helium coverage was used in the welding tank. The weld inter-pass temperature was held to ambient.

B. RESULTS

1. Radiographic

Fifteen of the 24 specimens exhibited varying degrees of gas porosity. The quality levels of the specimens based upon Specification ASTM-E-192-62T (see radiographic standards) are listed in Table XXVI.

2. Mechanical Properties

The results of mechanical property tests are listed in Table XXVII. The comparative properties of the titanium alloy vane-section and the 7079-T652 fuel inducer (center-section properties) are shown in Figures No. 17, No. 18, and No. 19.

The vane-section is notch-tough, at stress concentration, K_t to 6.3, based upon notch-tensile and notch-yield criteria. The titanium alloy is seen to have higher strength and ductility than the 7079-T652 aluminum alloy. More important, notch-toughness of the titanium alloy is retained down to -423°F. This is not true for the 7079-T652 aluminum alloy. The 0.2% offset yield strength-to-density ratios are also higher for the cast 5Al-2.5Sn-ELI grade (see Figure No. 19).

3. Macrostructure and Microstructure

Figure No. 20 is a photomacrograph of the vane. The structure of the vane is coarse, as expected for a casting. The weld repair has larger grains than the vane and is sound.

TABLE XXVI

RADIOGRAPHIC INSPECTION DATA FOR PUMP INDUCER CASTING
(VANE SECTION)

<u>Tensile Specimen</u>	<u>Condition</u>	<u>Quality Level per ASTM E 192-62T</u>
1	No defect	-
2	Gas porosity	1
3	Gas porosity	1
4	Gas porosity	2
5	Gas porosity	1
6	Gas porosity	6
7	No defect	-
8	No defect	-
9	Gas porosity	5
10	Gas porosity	3
11	No defect	-
12	Gas porosity	2
13	No defect	-
14	No defect	-
15	No defect	-
16	Gas porosity	7
17	Gas porosity	1
18	Gas porosity	2
19	Gas porosity	8
20	No defect	-
21	Gas porosity	8
22	Gas porosity	5
23	Gas porosity	7
24	No defect	-

TABLE XXVII

MECHANICAL PROPERTIES OF 5Al-2.5Sn ELI TITANIUM ALLOY PUMP INDUCER CASTING
(VANE SECTION)

Tensile Specimen	Specimen Orientation	Test Temp (°F)	Ultimate Strength (ksi)	0.2% Offset Yield Strength (ksi)	Elongation (% in 4D)	Reduction of Area (%)	Notch Tensile Strength (ksi)	Notch Tensile Ratio	Notch Yield Ratio	Root Radius (in.)	Stress Conc. (K_t)
2	Radial	R.T.	114.5	105.4	12.0	27.5					
4	Radial	R.T.	112.1	104.3	11.0	22.6					
		Avg.	113.3	104.9	11.5	25.1					
8	Radial	R.T.	Notched	Tensile Specimen			159.2			0.0011	9.5
9	Radial	R.T.	Notched	Tensile Specimen			158.7			0.0020	6.3
		Avg.					158.9	1.40	1.52		
14	Tangential	R.T.	110.7	101.6	11.0	21.1					
16	Tangential	R.T.	109.6	99.5	8.5	18.9					
		Avg.	110.2	100.6	9.8	20.0					
21	Tangential	R.T.	Notched	Tensile Specimen			158.2			0.0019	6.3
24	Tangential	R.T.	Notched	Tensile Specimen			158.1			0.0021	6.3
		Avg.					158.1	1.44	1.58		
3	Radial	-320	181.4	156.9	10.0	14.0					
15	Tangential	-320	180.3	151.4	10.0	16.2					
11	Radial	-320	Notched	Tensile Specimen			232.0	1.28	1.48	0.0022	6.3
22	Tangential	-320	Notched	Tensile Specimen			222.1	1.23	1.47	0.0020	6.3
1	Radial	-423	190.0	161.8	6.5	14.1					
5	Radial	-423	194.8	164.0	5.5	10.9					
		Avg.	192.4	162.9	6.0	12.5					
7	Radial	-423	Notched	Tensile Specimen			221.5			0.0021	6.3
10	Radial	-423	Notched	Tensile Specimen			228.0			0.0015	6.3
12	Radial	-423	Notched	Tensile Specimen			216.0			0.0015	6.3
		Avg.					221.8	1.15	1.36		

TABLE XXVII (Cont'd)

Tensile Specimen	Specimen Orientation	Test Temp (°F)	Ultimate Strength (ksi)	0.2% Offset Yield Strength (ksi)	Elongation (% in 4D)	Reduction of Area (%)	Notch Tensile Strength (ksi)	Notch Tensile Ratio	Notch Yield Ratio	Root Radius (in.)	Stress Conc. (K_t)
13	Tangential	-423	192.0	161.8	6.5	14.1					
17	Tangential	-423	192.9	152.5	8.5	14.8					
18	Tangential	-423	190.5	155.8	4.0	13.2					
		Avg.	191.8	156.7	6.3	14.0					
19	Tangential	-423	Notched	- Tensile Specimen			217.2			0.0013	8.8
20	Tangential	-423	Notched	- Tensile Specimen			216.5			0.0018	6.3
23	Tangential	-423	Notched	- Tensile Specimen			225.9			0.0012	9.1
		Avg.					219.9	1.15	1.40		

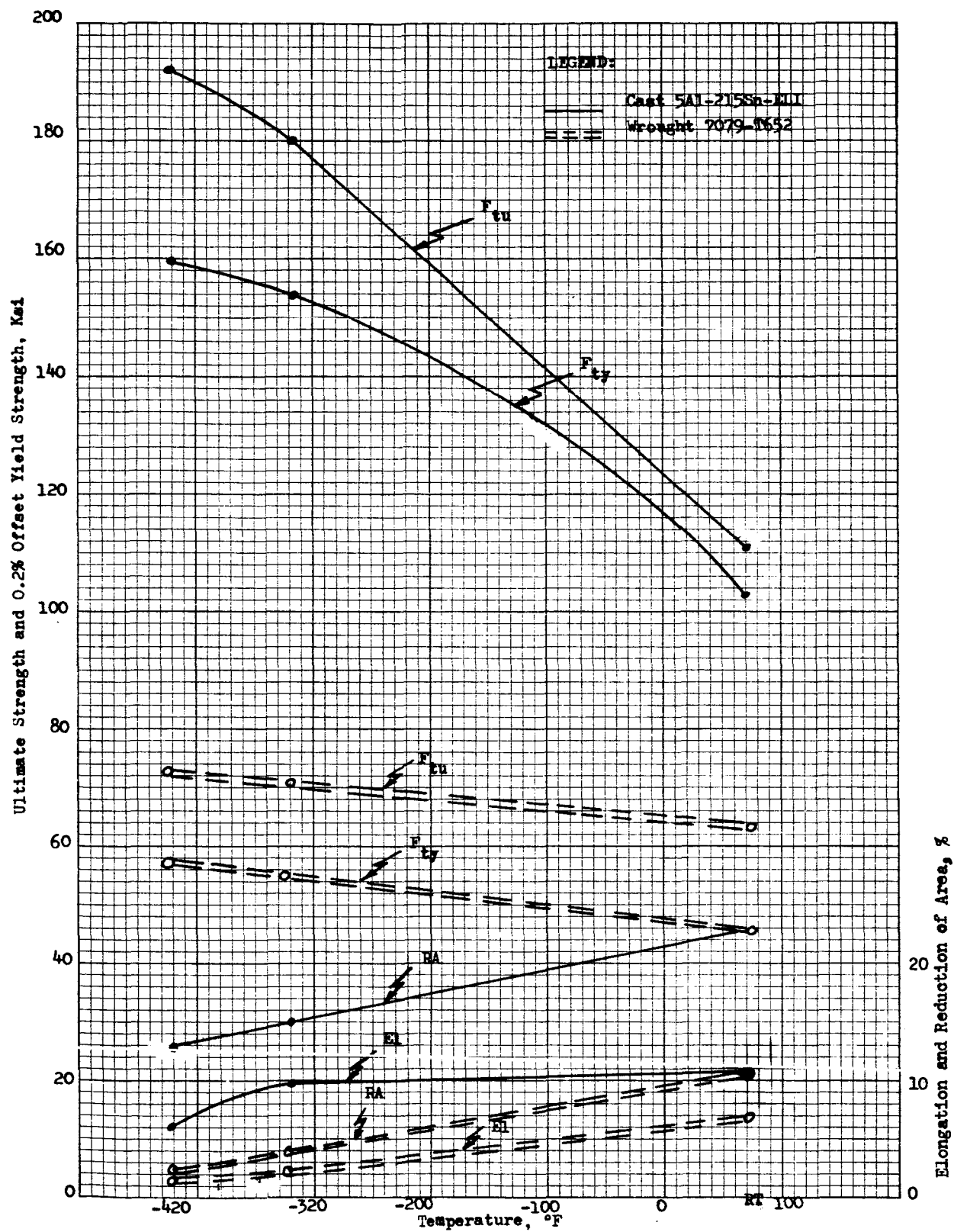


Figure 17

Mechanical Properties of Cast Ti-5Al-2.5Sn-ELI and
7079-T652 Aluminum Pump Inducers

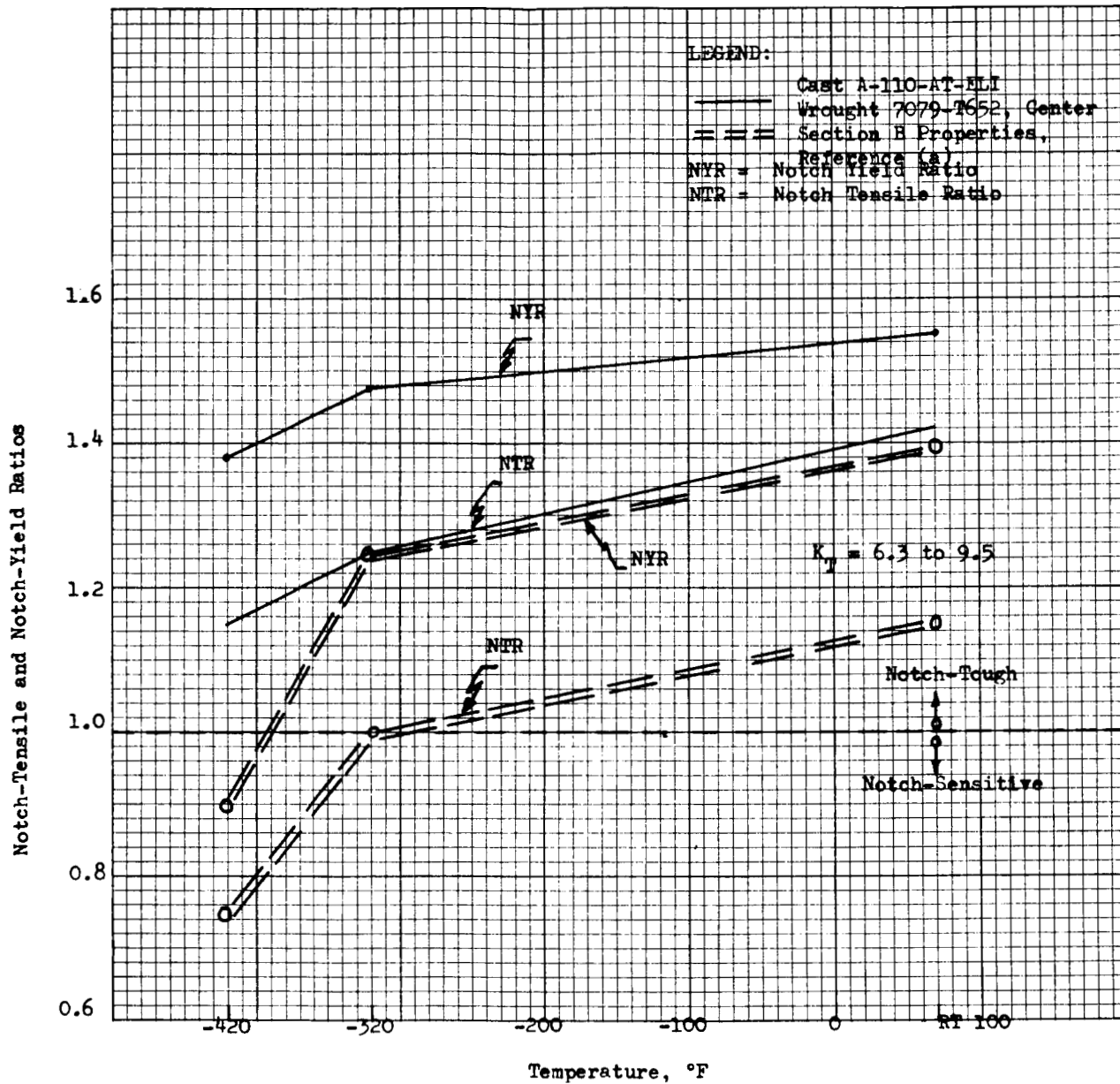


Figure 18

Notch Tensile and Notch-Yield Ratios of Cast Ti-5Al-2.5
Sn-ELI and 7079-T652 Aluminum Pump Inducers

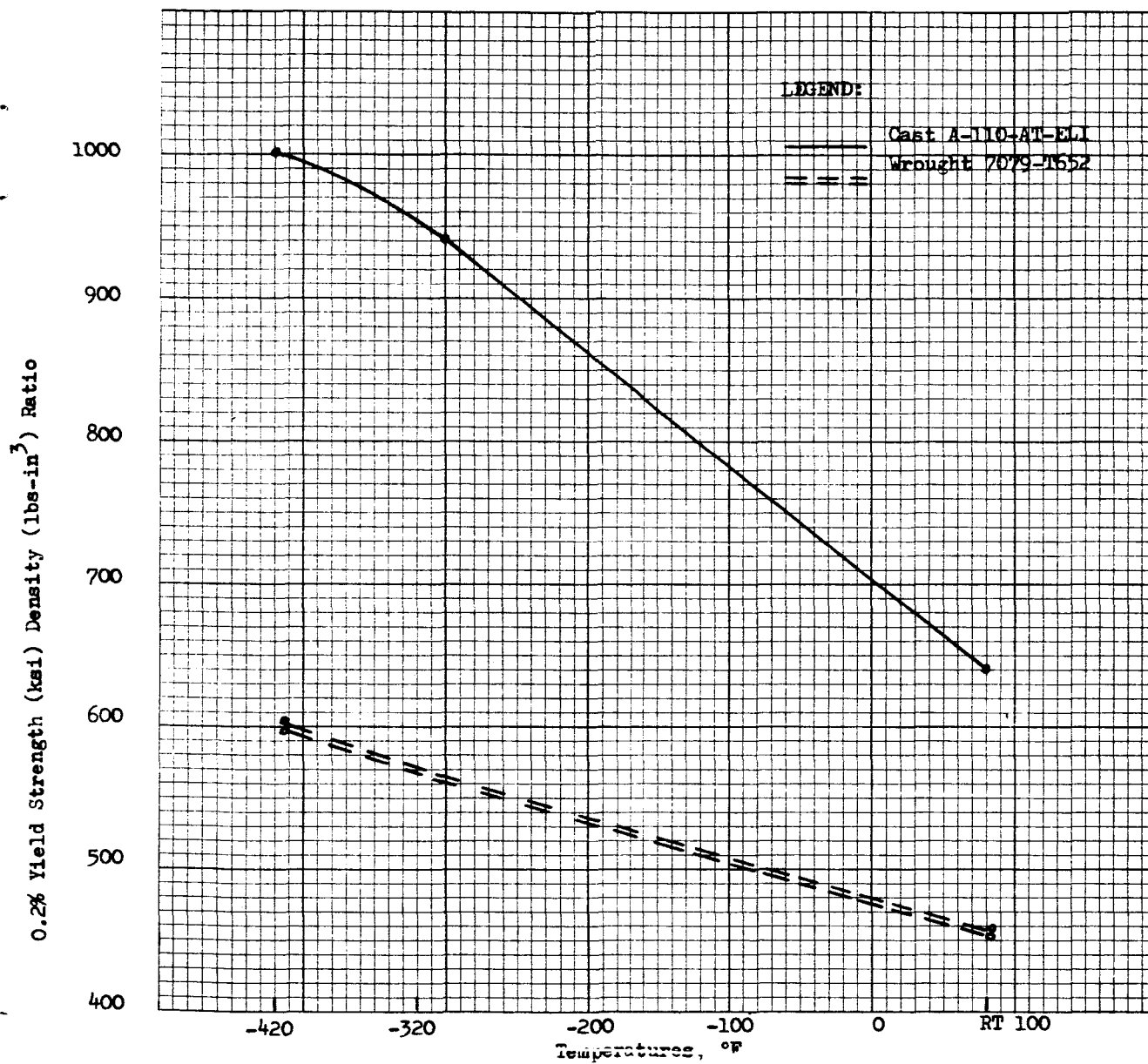


Figure 19

0.2% Yield Strength-Density Ratio of Cast Ti-5Al-2.5
Sn-ELI and 7079-T652 Aluminum Pump Inducers

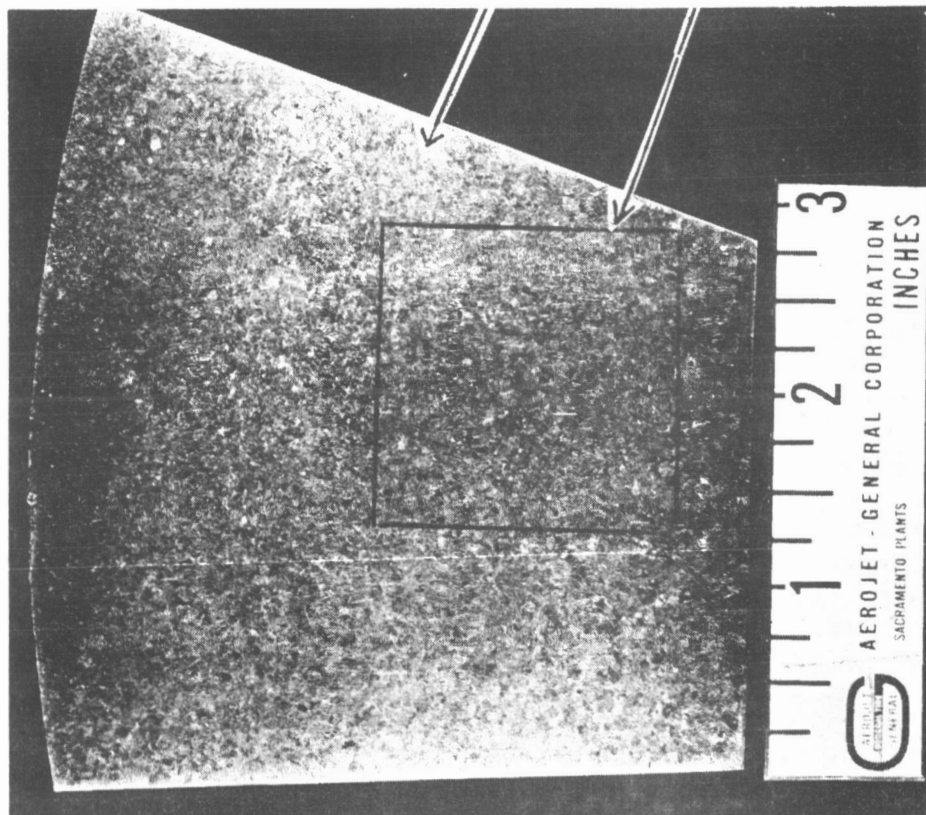


Figure 20

Macrostructure of Vane and Repair Weld in Vane

Magnification: 10X

Structure is coarse and shows a sound weld. Note the larger grain size of the weld as opposed to that of the parent metal.

Figure No. 21 is a photomicrograph of the vane (viewed in the transverse direction) at the mid-thickness. The view shows a coarse-grained dendritic structure.

Figure No. 22 is a photomicrograph of the vane surface area viewed transversely. The titanium-graphite mold interaction zone is approximately 0.018-in. deep based upon the hardness survey. Hardness (converted from Tukon) ranged from Rockwell C-38.2 at the surface (0.004-in.) to C-22.0 (0.018-in. from surface); TiC was not evident in the interaction zone, and the zone's carbon content was not presumed to exceed the solubility limit. In titanium, the carbon equilibrium solubility limit is given as 0.2% (by weight) based upon the phase diagram.

4. Chemistry

The results of a chemical analysis indicated that the interstitial limits are within the maximum values for the 5Al-2.5Sn-ELI grade (see Table XXVIII).

5. Weld Repair Study

The results of this study revealed that the weld repair in the vane-section is sound (Figure No. 20).

The weld repair, located at the hub-section between the vanes, cracked after welding (Figures No. 23, No. 24, and No. 25). The cracks are illustrated by dye penetrant. Three attempts were made to repair the cracks, and the defects extended in length. One crack propagated through the vane thickness (Figure No. 23, View 2). Hardness survey showed no contamination during welding. The welding schedule was revised to nearly equalize the heating and cooling rates in the weld area around the thin vane and massive hub section. This procedure resulted in the sound weld joint (Figure No. 26). The cracking at the dissimilar thickness zone results from thermal stresses established because of uneven cooling and heating rates.

The tests serve to illustrate that the cast titanium alloy is repair-weldable using proper procedures. This is a definite advantage over the non-weldable 7079 aluminum alloy for the fuel inducer application.

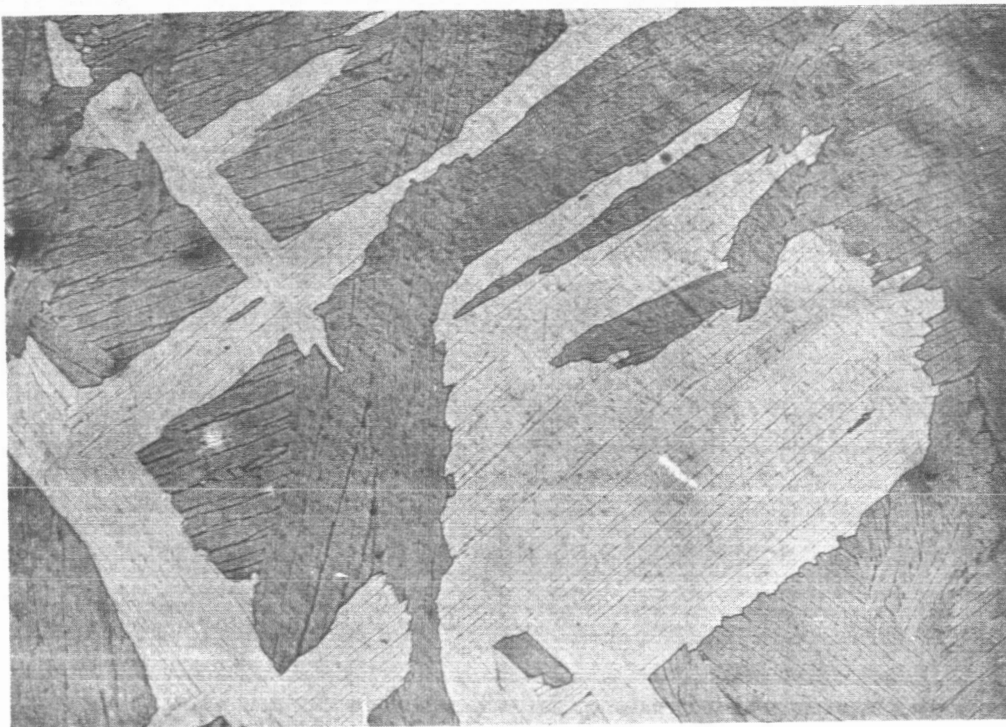
C. CONCLUSIONS

1. The cast Ti-5Al-2.5Sn-ELI titanium alloy vane section exhibited high 0.2% offset yield strength, good ductility, and high notch-toughness in the room to -423°F temperature range.
2. The cast alloy can be repair-welded.
3. The vane section exhibited excessive gas-porosity.

TABLE XXVIII

CHEMICAL COMPOSITION OF EXPERIMENTAL
M-1 FUEL PUMP IMPELLER CASTING
OF TITANIUM ALLOY 5Al-2.5Sn ELI

<u>Element</u>	<u>SKD-C291 Casting</u> <u>(%)</u>	<u>Recommended ELI</u> <u>Chemistry for</u> <u>5Al-2.5Sn-ELI</u>
Carbon	0.032	0.05 max.
Aluminum	5.3	4.75 - 5.75
Tin	2.7	2.2 - 2.8
Iron	0.20	0.25 max.
Oxygen	0.10	0.12 max.
Hydrogen	0.0030	0.0125 max.
Nitrogen	0.010	0.04 max.
Manganese	Less than 0.05	0.10 max.
Vanadium	Less than 0.10	0.10 max.
Molybdenum	Less than 0.10	0.10 max.
Chromium	Less than 0.10	0.10 max.
Titanium	Remainder	Remainder

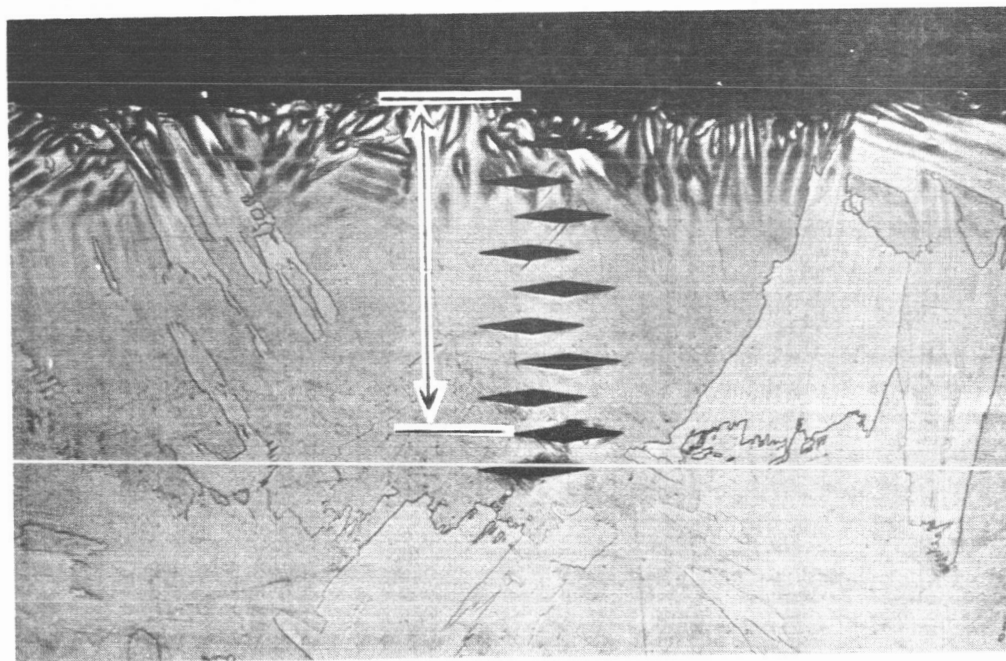


Etchant: Keller's

Magnification: 100X

Figure 21. Microstructure of Vane Section

The structure is coarse and dendritic. This is the transverse view of the threaded portion of tensile specimen number 6.

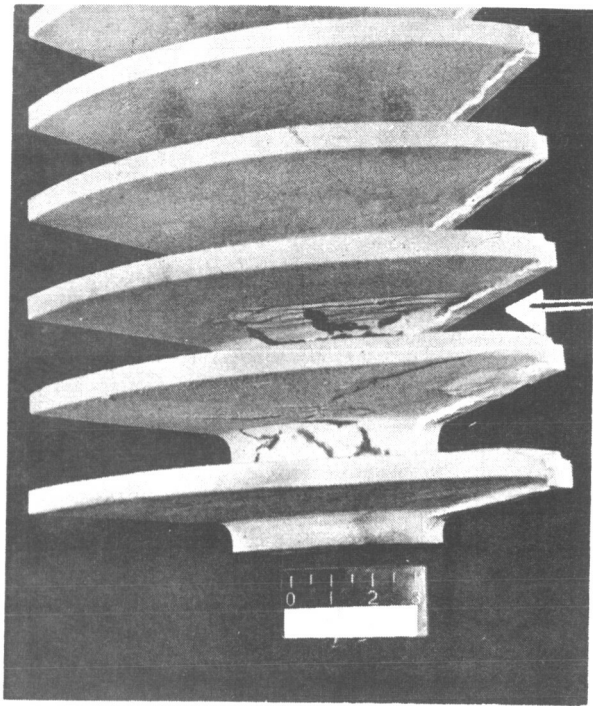


Etchant: Keller's

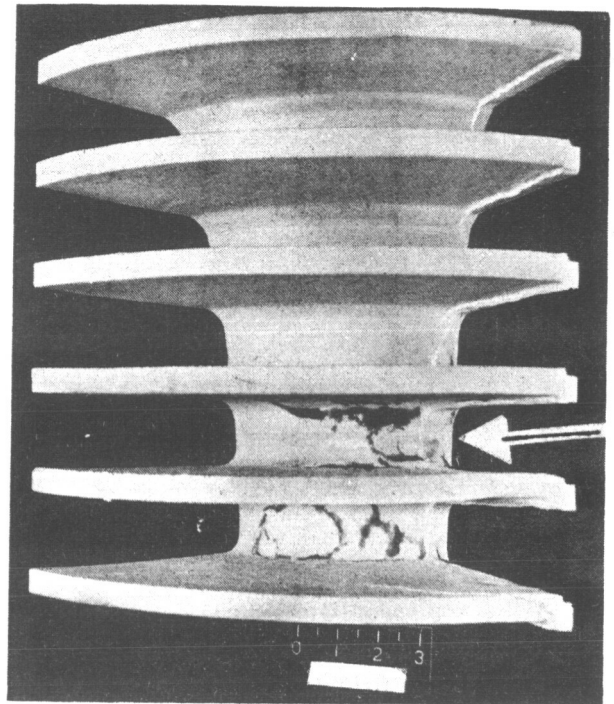
Magnification: 100X

Figure 22. Titanium Alloy - Graphite Mold Reaction Zone

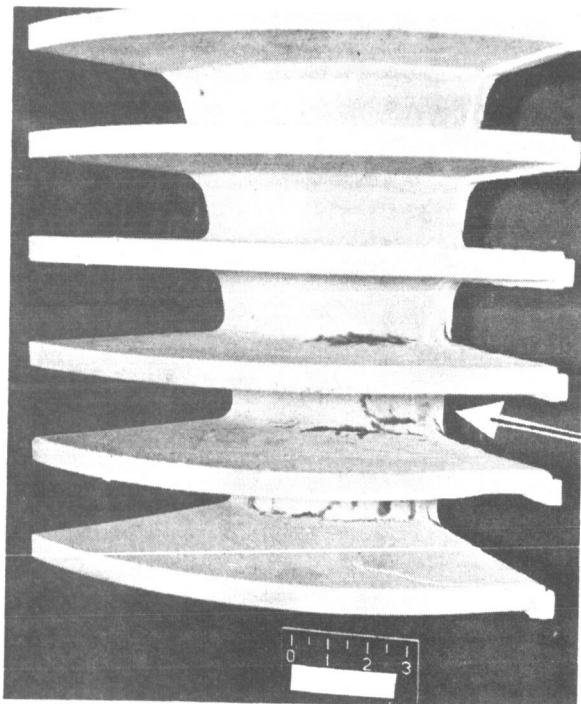
The reaction zone is 0.018 inch thick. Hardnesses from surface to core (converted to Rockwell C) = 37.2, 38.2, 34.4, 31.8, 28.1, 28.4, 25.2, 24.7, 22.0, and 22.6.



View 1



View 3



View 2

The cracks (arrows) are located at the junction between the vanes and hub section. They are caused by stresses arising from the unequal heating and cooling rates during the welding operation.

Figure 23

Cracked Welds in Dye-Penetrant Condition

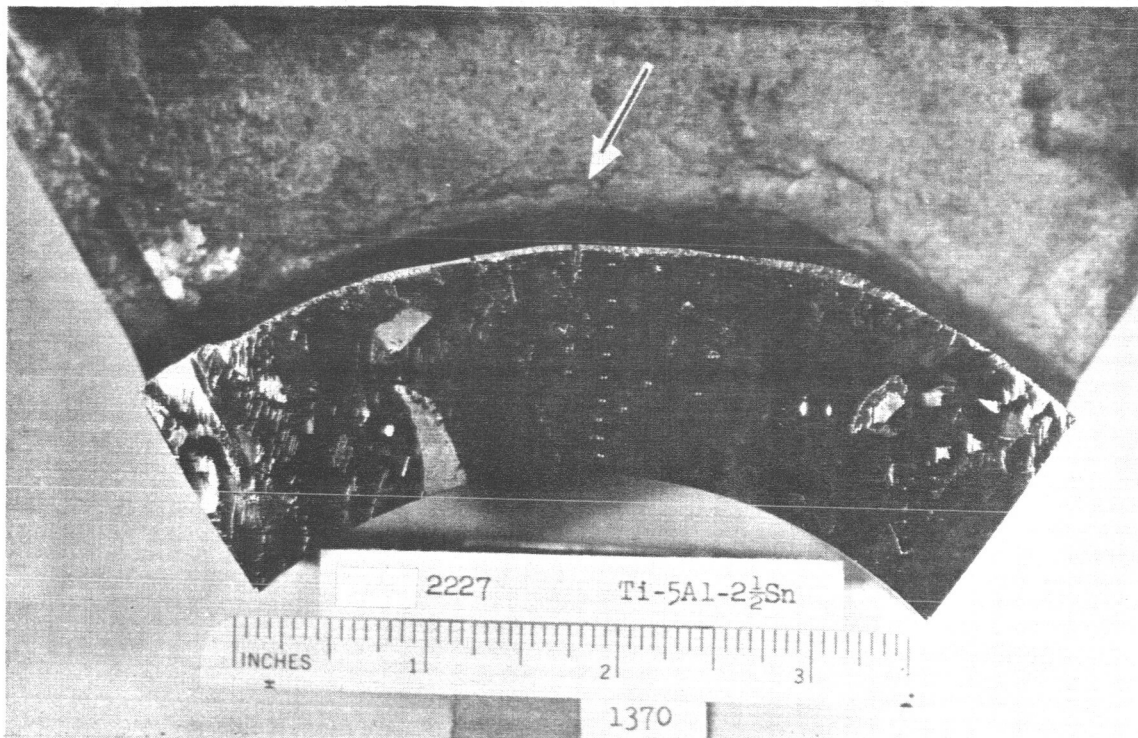


Figure 24. Cracked Weld in Macro-Etched Condition.

The crack (arrow) is exposed by cutting between the vanes. Note again the large grain size of the casting. The indentations are hardness impressions.

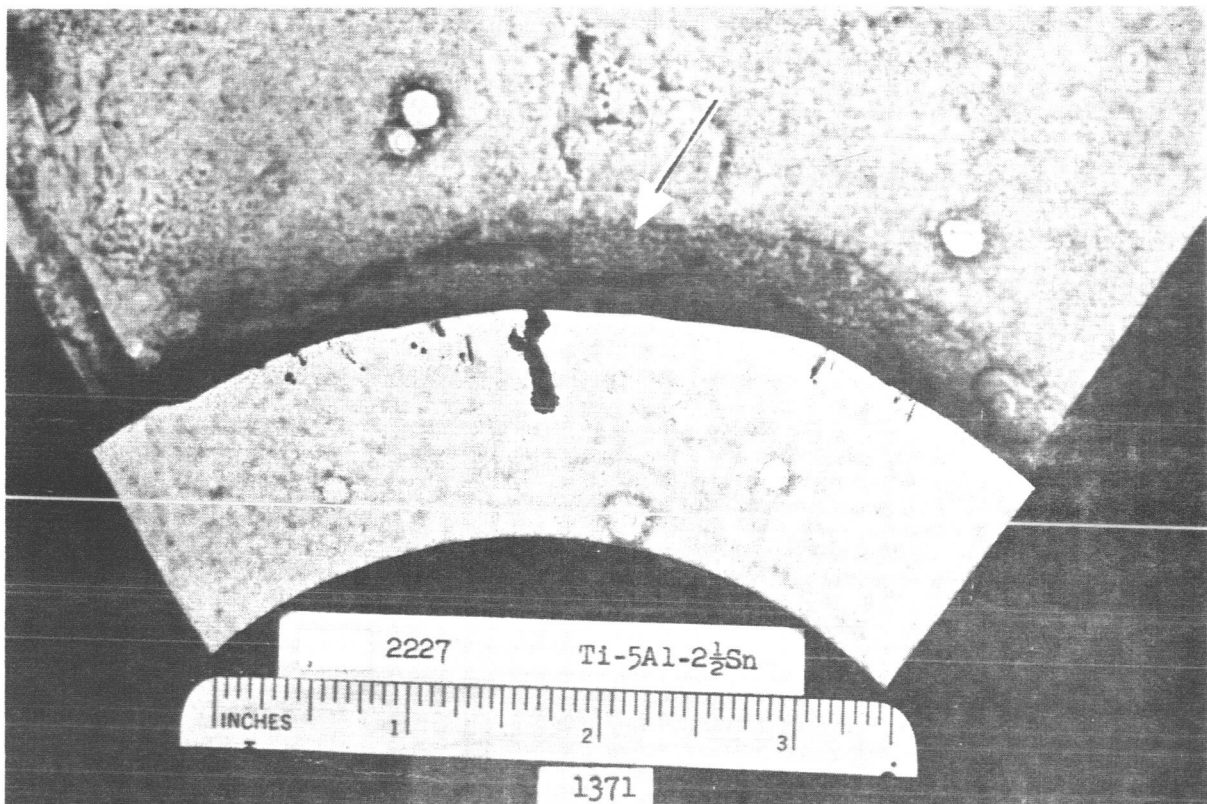
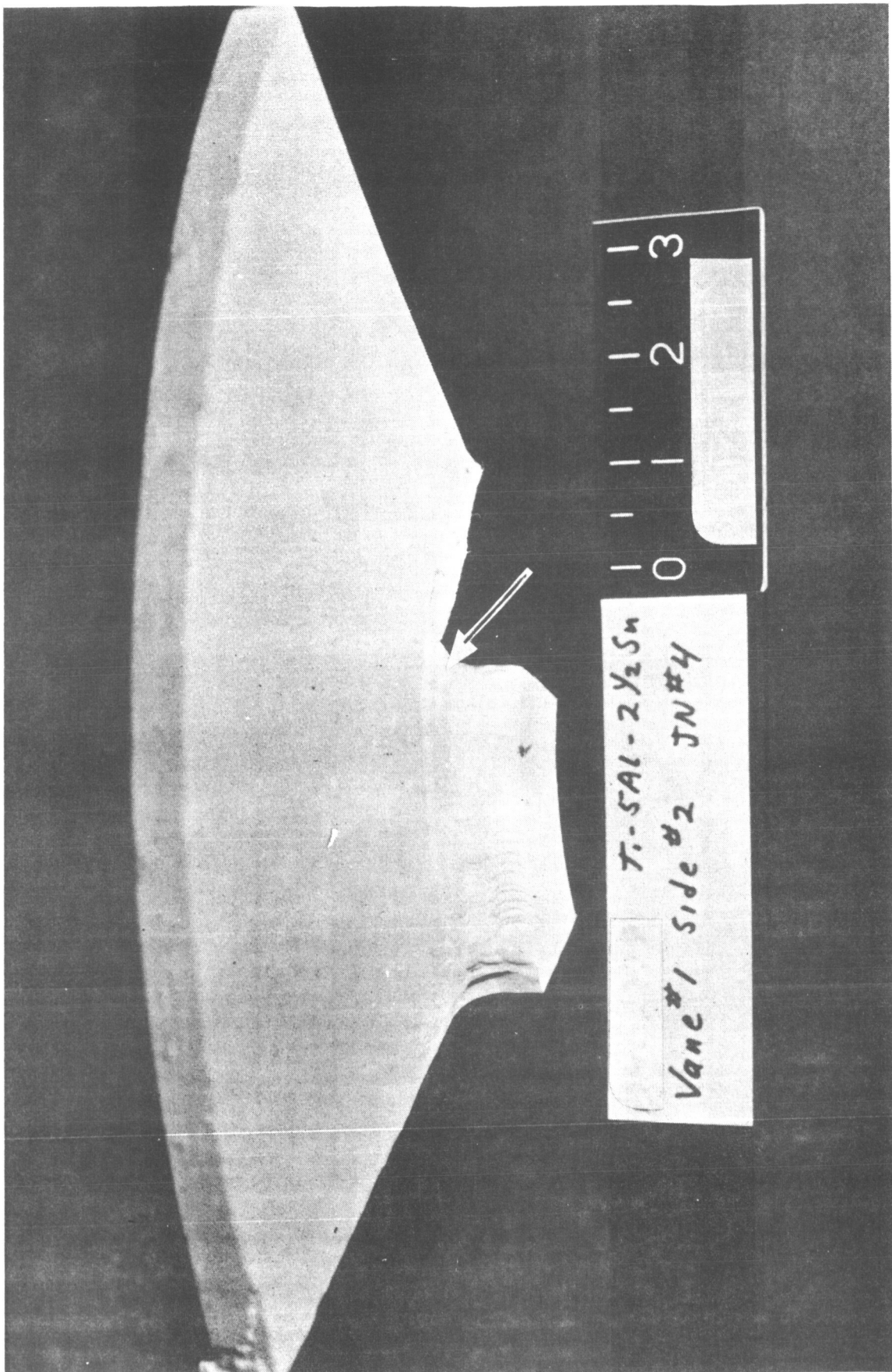


Figure 25. Cracked Weld in Dye-Penetrant Condition.

Note the bleed-out.



The weld is sound. Cracking is prevented by minimizing thermal stresses during the welding operation.

Figure 26

Sound Weld in Dye-Penetrant Condition

4. The cast titanium alloy appears superior to the currently used Type 7079-T652 aluminum alloy for the fuel inducer application. It has superior low temperature strength and ductility as well as notch-toughness. The 0.2% offset yield strength-to-density ratio is also higher.

D. RECOMMENDATIONS

1. Evaluate the vanes for fatigue strength in the room temperature to -423°F range.

2. Establish the hub section mechanical properties in the room temperature to -423°F range.

3. Study alloy machinability.

4. Provided results of the additional tests are satisfactory, produce a second casting for fabrication into a finished part for engine tests.

BIBLIOGRAPHY

1. Gustafson, K. L., Development and Evaluation of Braze Alloys for Vacuum Furnace Brazing, Aerojet-General Report No. 8800-26, 5 November 1965
2. Hofmann, W. and Rauls, W., Neue Beobachtungen Zur Versprödung Von Stahl Durch Wasserstoffeinwirkung Bei Raumtem Peratur, Dechema-Monographien NR. 734-760, 1962
3. Hunt, V., Induction Processed Separable Tubular Brazed Connectors, Aerojet-General Report No. 8800-24, 5 November 1965
4. Inouye, F. T., Properties of Large 7079 Aluminum Forgings, Aerojet-General Report No. 8800-20, 9 February 1966
5. Inouye, F. T., Hunt, V., Janser, G. R., and Frick, V., Summary of Experience Using Inconel 718 on M-1 Engine, Aerojet-General Report No. 8800-37, 30 December 1966

REPORT NASA CR 54961 DISTRIBUTION LIST

W. F. Dankhoff (5 Copies)
NASA
Lewis Research Center
21000 Brookpark Road
Cleveland, Ohio 44135
Mail Stop 500-305

J. A. Durica (1 Copy)
Mail Stop 500-210

Patent Counsel (1 Copy)
Mail Stop 77-1

Lewis Library (2 Copies)
Mail Stop 60-3

Lewis Technical Information
Division (1 Copy)
Mail Stop 5-5

Office of Reliability and
Quality Assurance (1 Copy)
Mail Stop 500-203

J. J. Lombardo (1 Copy)
SNPO-C
Mail Stop 5-1-1

W. W. Wilcox (1 Copy)
Mail Stop 500-305

G. Zalabek (1 Copy)
Mail Stop 500-305

D. D. Scheer (1 Copy)
Mail Stop 500-305

L. Weise (1 Copy)
Mail Stop 500-120

W. A. Tomazic (1 Copy)
Mail Stop 500-305

J. Kazaroff (5 Copies)
Mail Stop 500-305

W. E. Russell (2 Copies)
Mail Stop 14-1

NASA
Scientific and Technical
Information Facility (6 Copies)
Technical Information Abstracting and
Dissemination Facility
Box 5700
Bethesda, Maryland

Library (1 Copy)
NASA
Ames Research Center
Moffett Field, California 94035

Library (1 Copy)
NASA
Flight Research Center
P. O. Box 373
Edwards AFB, California 93523

Library (1 Copy)
NASA
Goddard Space Flight Center
Greenbelt, Maryland 20771

Library (1 Copy)
NASA
Langley Research Center
Langley Station
Hampton, Virginia 23365

Library (1 Copy)
NASA
Manned Spacecraft Center
Houston, Texas 77058

Library (1 Copy)
NASA
George C. Marshall Space Flight
Center
Huntsville, Alabama 35812

Library (1 Copy)
NASA
Western Operations Office
150 Pico Boulevard
Santa Monica, California 90406

Library (1 Copy)
Jet Propulsion Laboratory
4800 Oak Grove Drive
Pasadena, California 91103

A. O. Tischler (2 Copies)
NASA
Washington, D. C. 20546

J. W. Thomas, Jr. (5 Copies)
NASA
George C. Marshall Space Flight
Center, I-E-E
Huntsville, Alabama 35812

Dr. E. B. Konecni (1 Copy)
NASA
Executive Office of the President
Executive Office Building
Washington, D. C.

E. W. Broache (2 Copies)
Westinghouse Electric Corporation
Defense Division
Materials and Processes Engineering
Baltimore, Maryland

C. E. Cataldo (2 Copies)
R-P&VE-MM
NASA
George C. Marshall Space Flight
Center
Huntsville, Alabama 35812

E. A. Lange (2 Copies)
Code 6381
U. S. Naval Research Laboratory
Washington, D. C. 20390

Library (2 Copies)
Batelle Memorial Institute
Columbus, Ohio